Measurement of 1/*f* Noise in Carbon Composition and Thick Film Resistors

Patrick Barry and Steven Errede

University of Illinois at Urbana-Champaign, Department of Physics

Technical Abstract

Thermal noise and 1/*f* noise are known to exist in carbon composition (CC) and thick film (TF) resistors. A circuit involving a differential instrumentation op-amp was used to measure the noise of a resistor under test. The noise spectra of these resistors were measured using a dynamic signal analyzer that performs an auto-correlation Fourier transform from the time domain to the frequency domain to determine the amount of 1/*f* noise in the spectra. Various noise-canceling techniques were implemented, such as nitrogen inerting a grounded metal box containing the circuit. A dc voltage was applied across the resistor under test in each measurement. The results show that CC and TF resistors produce 1/*f* noise and have a voltage dependence on the noise, which varies as $1/V_{dc}^{\gamma}$. The exponent *γ* was determined for each 1/*f*-noise-producing resistor. The resistors produce an ac noise power in the zeptowatt/Hz-attowatt/Hz range (10^{-21}-10^{-18} Watts/Hz). In the future, additional thermal noise measurements and analysis will be carried out on resistors, in addition to building a 1/*f*-noise-producing guitar effects pedal.

Non-technical Abstract

Thermal noise, which is the electromagnetic signal associated with thermal agitation of electrons, is present in all resistors and represented by the noise spectral function, which is dependent on temperature and the resistance. In addition, 1/*f* noise is present in carbon composition (CC) and thick film (TF) resistors, where *f* represents the frequency. In the frequency domain, the level of 1/*f* noise decreases as frequency increases. A circuit was built to measure the spectral noise level of a resistor. Since the level of this noise was very small, various external noise sources were minimized. Various dc voltages were applied across the resistor, and as the dc voltage increased, the noise levels increased. The amount the noise levels differed for the different resistors was also measured. In the future, further resistor thermal noise measurements and analysis will be performed, in addition to building a 1/*f*-noise-producing guitar effects pedal.

I. Introduction

I.1. What is Noise?

Noise can be described as any unwanted signal. While unwanted, noise is a very real and intrinsic property of any electronic system. In electronic systems, noise includes contributions from mechanical interference, electrical interference, fluctuations in the ambient electromagnetic field, and fluctuations in electron movement [1]. Generally, noise limits the overall performance of the system [2]. Noise has been a popular research area and is a well-known topic.

Electronic equipment and even rooms have electromagnetic noise associated with them. Ambient electronic noise present in the lab room is shown from the oscilloscope trace depicted in **Figure 1-1**.

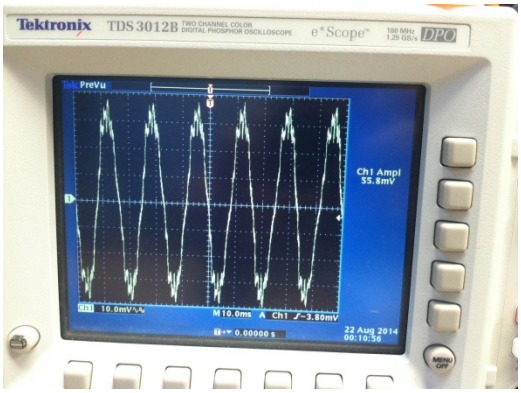

Figure 1-1*: An example of ambient noise as shown on the oscilloscope.*

In addition, other electromagnetic noise can emanate from electronic equipment, as well as fluorescent lights, as shown in **Figure 1-2**.

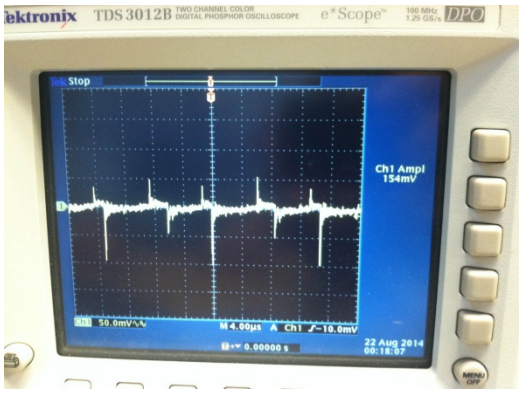

Figure 1-2*: An example of noise from a fluorescent light source as shown on the oscilloscope.*

As can be seen by these two figures, noise is not exactly periodic, attributable to the unwanted harmonics. Some noise processes are caused by random fluctuations in electromagnetic fields, noise curves can be shaky. Consequently, taking averages of many noise signals is required to understand a true pattern. Other well-known sources of noise are thermal noise and flicker (1/*f*) noise.

Thermal noise, also known as Johnson noise or Johnson-Nyquist noise or white noise, is a voltage due to agitation of charge carriers that are in thermal equilibrium with its environment [3]. The Nyquist theorem says that the noise spectral density in resistors in units of the mean-square voltage per unit frequency is $S_{V^2}(f) = 4k_BTR$, where k_B is Boltzmann's constant (k_B = 1.38 ×10^{-23} Joules/Kelvin), T is the absolute temperature of an object, and R is the resistance. Thermal noise is flat in frequency, as there is no f dependence in the noise spectral density. Random correlations among the charge carriers occur in the time domain.

Flicker noise, or 1/*f* noise, is a type of noise that is proportional to the inverse of frequency. At low frequencies, the noise is the highest, and the noise decreases as frequency increases. Since frequency and time are inversely proportional, low frequencies correspond with long time scales. Correlations among charge carriers exist over long time scales in 1/*f*-noise producing systems. In addition to Johnson's measurements of flat-frequency thermal noise, he also measured 1/*f* noise at low frequency [4]. The noise spectral density associated with 1/*f* falls as 1/*f*. On a log-log plot, the noise

spectral density of 1/*f* noise is a straight line with slope = −1. While many measurements have been carried out and many theories have been proposed, no one theory uniquely describes the physics behind 1/*f* noise. Dutta and Horn have proposed theories of the physical cause of 1/*f* noise, such as activated random processes inside the resistor, diffusion, and noise from bremsstrahlung [5]. The majority of the experiments and the focus of this thesis deal with measuring 1/*f* noise in resistors.

I.2. How does 1/*f* noise pertain to music?

Voss and Clarke examined the spectral density of frequency fluctuations associated with audio signals broadcast from radio stations, such as classical, jazz, blues, and rock music, and news and talk, which all followed a 1/*f* noise pattern [6]. Speech patterns and cognitive functions have also been associated with 1/*f* noise [7]. In addition, raindrops fall as a 1/*f* pattern and blood flow through veins follows a 1/*f* pattern. Because humans relate well to 1/*f* noise, it has musical implications.

I.3. What produces 1/*f* noise?

Carbon composition (CC) and thick-film (TF) resistors are known to produce 1/*f* noise [8]. Carbon composition resistors were heavily used in the early to mid 20thcentury and are found in vintage tube amplifiers. Other devices, such as Zener diodes, also produce 1/*f* noise at low frequencies. In the following experiments, CC and TF resistors were tested for their 1/*f* noise contributions.

I.4. Motivation behind testing CC resistors

In the physics of music laboratory at the University of Illinois at Urbana-Champaign, vintage tube amplifier circuitry has been studied in detail. As shown in **Figure 1-3**, vintage tube amplifiers, specifically a Fender Bassman Model 5F6-A, used 100-kΩ CC resistors as plate-load resistors, which are frequently used in the preamplifier circuits of many tube amplifiers.

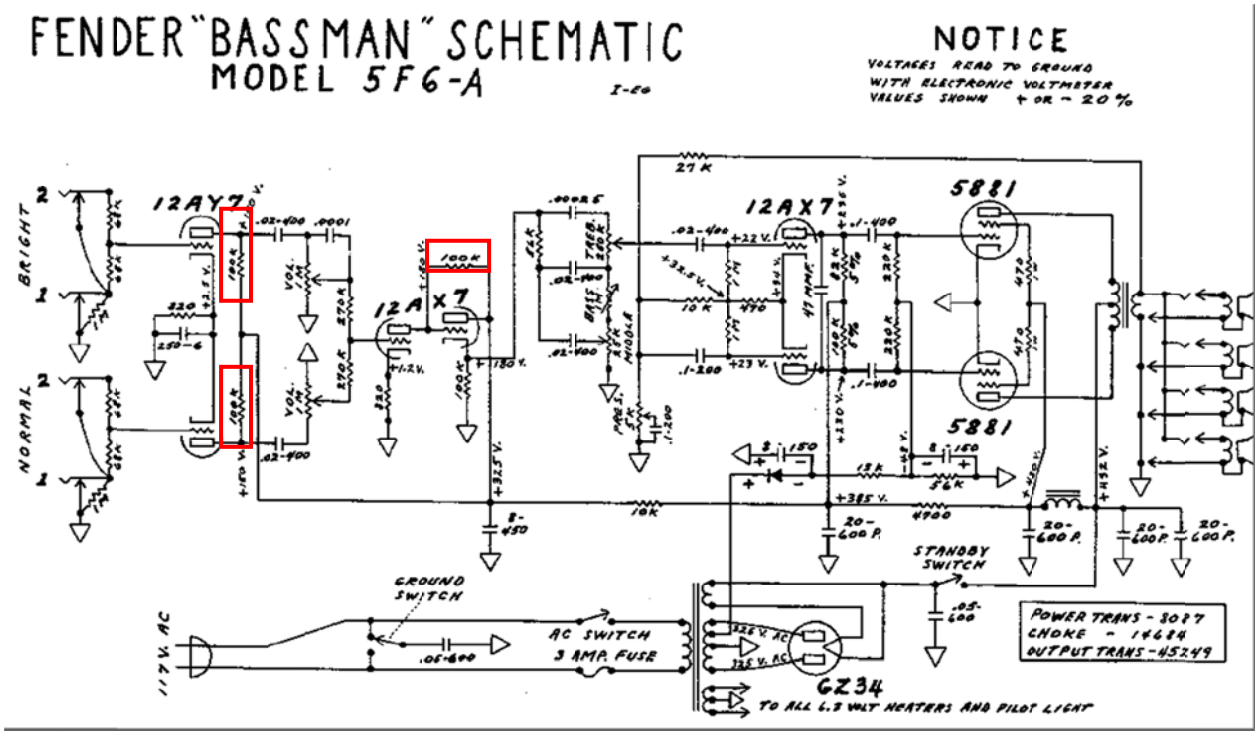

***Figure 1-3**: The schematic of a Fender Bassman Model 5F6-A. The red-highlighted resistors have resistances of 100 kΩ and are used as plate-load resistors.*

I.5. The resistors

Before measuring noise spectra for CC resistors, the noise spectra of metal film (MF) resistors were measured to establish the accuracy of the circuit due to their well-defined thermal noise contribution. All of the resistors that were tested had resistances of 100 kΩ. Old stock (OS) CC resistors were tested of power ratings ½ W, 1 W, 2 W. A high reliability (Hi-Rel) OS CC 1-W resistor was also tested. Other resistors such as 1-W TF resistor, 1-W MF resistor, and new stock (NS) CC 1-W resistor were also tested. **Figure 1-4** shows the resistors that were tested.

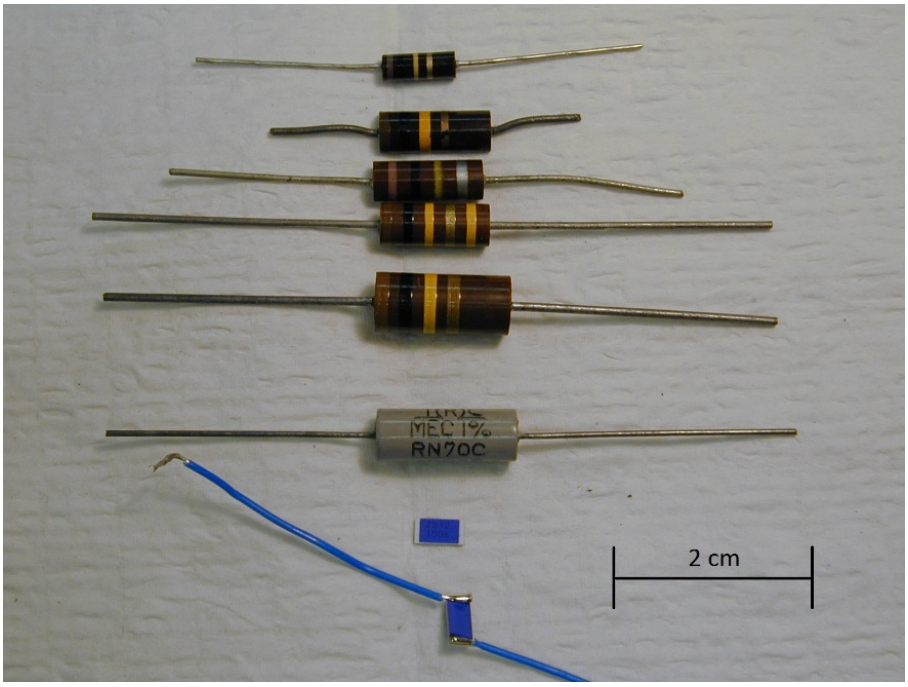

Figure 1-4: *From top to bottom: 1/2-W OS CC, 1-W OS CC, 1-W NS CC, 1-W OS High-reliability CC, 2-W OS CC, 1-W MF, 1-W TF, 1-W TF with leads*

II. Methods

II.1. Experimental Setup

A schematic of the 1/*f* noise-producing circuit that we designed and built is shown in **Figure 2-1**. The circuit was built to measure the noise of the resistor under test (Rdut). Each resistor measured for its 1/*f*-noise contribution was placed at R3 as shown in **Figure 2-1**.

The circuit components V1 and V2 in **Figure 2-1** are a positive and negative dc power supply, which provided the dc voltage applied to the resistor under test. R1, R2, and R3 were all chosen to have 100 kΩ of resistance such that the voltage drop across each resistor was the same. The components C1 and C2 are blocking capacitors that pass only an ac signal. Along with the resistors R4 and R5 (R4 associated with C1 and R5 associated with C2), the blocking capacitors form a high pass filter that blocks frequencies lower than $f_c = \frac{1}{4\pi}\ Hz$. The frequency information from the ac signal (which would not be available from the dc component) is essential in evaluating the frequency dependence of the noise spectra.

Components of the circuit were chosen to minimize ambient noise of the circuit. R1 and R2 were specifically chosen to be metal film (MF) resistors, which are known to produce only Johnson-Nyquist (thermal) noise [9]. This Johnson-Nyquist, or white, noise is flat across the frequency spectrum; i.e., it does not produce 1/*f* noise. Because these resistors don't produce 1/*f* noise, they are ideal for a circuit used to measure the 1/*f* noise in only one component.

The AD624 is a low-noise and high-precision instrumentation op-amp used in the circuit to amplify and process the differential voltage signals from the positive and negative inputs [10]. Differential amplifiers have a common-mode rejection of coherent signals present at both the positive

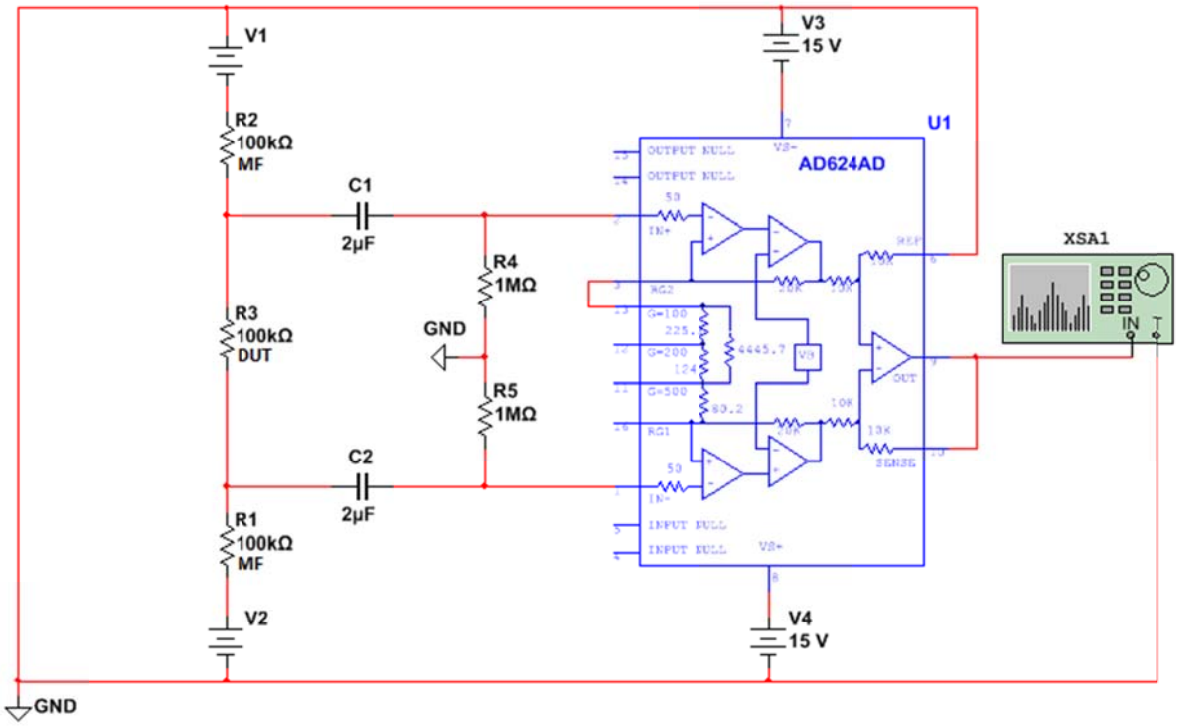

Figure 2-1: *A schematic of the circuit built to measure the noise of the device under test (Rdut) at R3*

and negative inputs; i.e., the common signals will cancel in the amplifier. The low-noise component to the AD624 makes it an ideal op-amp to use in the sensitive noise spectra measurements for this experiment. The gain on the op-amp was set to 100. Thus, the noise floor of the AD624 circuit is noisier than the intrinsic noise floor of the Agilent 35670A dynamic signal analyzer (DSA). Other specifications of the AD624 can be found in the datasheet [10].

A standby switch was also added to the circuit, temporarily shorting the AD624 inputs to ground. When changing the voltage on the power supplies, the transient signal output from the AD624 with a gain of 100 was very high. Early on in the experiment, an AD624 was destroyed, because of too rapidly changing the applied high voltage to the circuit. From that point on, a standby switch was used in the circuit to clamp the input signals of the op-amp to ground. Instead of the 1-MΩ resistors coupling with the 2-μF capacitors, 100-Ω resistors were connected to ground, which creates a much lower time constant for the voltage to dissipate to ground. This way, the AD624 was not overloaded when raising or lowering the HV.

II.2. The Agilent 35670A Dynamic Signal Analyzer

The Agilent 35670A DSA was used to analyze the noise signal output from the circuit. The DSA is represented by the component labeled "XSA1" in **Figure 2-1**. The DSA records the time-domain signal and produces a frequency-domain signal to produce a noise spectrum for analysis. The spectral noise data were saved in the DSA on its non-volatile random access memory (NVRAM) and then transferred to a computer via a USB cable.

The DSA reads in an analog time-domain signal, which it first converts to a digital time-domain signal. The DSA then performs an auto-correlation on this digital time-domain signal. The auto-correlation is a specialization of cross-correlation, which is the convolution of two complex functions involving complex conjugation. Auto-correlations take the cross-correlation of a function with respect to itself. The form for general auto-correlation is given below [11]:

$$\widetilde{\boldsymbol{h}}_{\boldsymbol{f}\star\boldsymbol{f}}(\boldsymbol{t}) \equiv \tilde{\boldsymbol{f}}(\boldsymbol{t}) \star \tilde{\boldsymbol{f}}(\boldsymbol{t}) = \tilde{\boldsymbol{f}}^{*}(-\boldsymbol{t}) \otimes \tilde{\boldsymbol{f}}(\boldsymbol{t}) = \int_{-\infty}^{\infty} \tilde{\boldsymbol{f}}^{*}(-\boldsymbol{\tau}) \cdot \tilde{\boldsymbol{f}}(\boldsymbol{t}-\boldsymbol{\tau}) \boldsymbol{d\tau} = \int_{-\infty}^{\infty} \tilde{\boldsymbol{f}}^{*}(\boldsymbol{\tau}) \cdot \tilde{\boldsymbol{f}}(\boldsymbol{t}+\boldsymbol{\tau}) \boldsymbol{d\tau}, \quad \textbf{(Eq. 2-1)}$$

where $\widetilde{\boldsymbol{h}}_{\boldsymbol{f}\star\boldsymbol{f}}(\boldsymbol{t})$ is the auto-correlation complex function in the time domain, and $\tilde{\boldsymbol{f}}(\boldsymbol{t})$is a complex time-domain signal.

However, the DSA cannot calculate an analytic expression in its digital system. A discrete Fourier transform is needed. The integrals in **Eq. 2-1** must become summations because of the digital nature of the computing method. In this experiment, the voltage in the time domain $\widetilde{\boldsymbol{V}}(\boldsymbol{t})$ is the function being auto-correlated. The result can be called $\widetilde{\boldsymbol{h}}_{\boldsymbol{V}\star\boldsymbol{V}}(\boldsymbol{t})$.

The DSA then calculates the frequency spectrum via fast Fourier transform (FFT) technique of the auto-correlated time signal. An FFT is a form of the Fourier transform that computes the discrete Fourier transform. In the frequency domain, the frequency dependence on a certain function can be considered. Since the noise spectrum of interest varies inversely with frequency, the frequency domain signal is needed. The general form of the Fourier transform is [11]:

$$\widetilde{\boldsymbol{g}}(\boldsymbol{f}) = \widetilde{\boldsymbol{g}}(\boldsymbol{\omega}) = \mathcal{F}\{\widetilde{\boldsymbol{g}}(\boldsymbol{t})\} \equiv \int_{-\infty}^{\infty} \widetilde{\boldsymbol{g}}(\boldsymbol{t}) \boldsymbol{e}^{-\boldsymbol{i\omega t}} \boldsymbol{dt} = \int_{-\infty}^{\infty} \widetilde{\boldsymbol{g}}(\boldsymbol{t}) \boldsymbol{e}^{-\boldsymbol{i2\pi ft}} \boldsymbol{dt}, \quad \textbf{(Eq. 2-2)}$$

where $\widetilde{\boldsymbol{g}}(\boldsymbol{f})$ is a complex frequency-domain signal, $\widetilde{\boldsymbol{g}}(\boldsymbol{\omega})$ is also a complex frequency-domain signal ($\omega \equiv 2\pi f$), and $\widetilde{\boldsymbol{g}}(\boldsymbol{t})$ is a complex time-domain signal. A more appropriate, discrete, version replaces the integrals in **Eq. 2-2** with summations.

Then, by the Weiner-Khintchine theorem [11], a frequency-domain noise spectrum is calculated. The DSA calculates the following noise spectrum

$$\boldsymbol{S}_{\boldsymbol{V}^2}(\boldsymbol{f}) = \frac{|V(f)|^2}{\boldsymbol{\Delta f}} = \frac{\boldsymbol{\alpha}}{\boldsymbol{f}^{\boldsymbol{\beta}}} \left[\frac{\boldsymbol{V^2}_{\boldsymbol{rms}}}{\boldsymbol{Hz}}\right], \quad \textbf{(Eq. 2-3)}$$

where $\boldsymbol{\alpha}$ is the frequency spectrum intercept at f = 1 Hz (i.e. when $\log_{10} 1 = 0$), $\boldsymbol{\beta}$ is the slope of noise spectrum vs. frequency on a log-log plot, and $\boldsymbol{\Delta f}$ is the frequency bin size on the DSA. The DSA processor takes into account $\boldsymbol{\Delta f}$ and presents $\boldsymbol{S}_{\boldsymbol{V}^2}(\boldsymbol{f})$ in $\frac{V^2 rms}{Hz}$.

Specific settings were applied to the DSA to carry out the spectral noise measurements. The human audio frequency range is about 20 Hz–20 kHz, thus we chose the frequency span of the DSA to be B_w = 25.6 kHz, starting at 32 Hz and ending at 25.632 kHz, where B_w is the bandwidth. The number of resolution lines was set to 1600, so 1601 frequency data points were measured for each spectrum. The frequency bin size, $\boldsymbol{\Delta f}$ in **Eq. 2-3**, was 16 Hz.

The time to carry out a frequency range is $\tau = \frac{\boldsymbol{1}}{\boldsymbol{2\pi B_w}}$. Thus, for B_w = 25.6-kHz frequency span, the time for one scan is τ = 6.21 μs. Since it takes such a short time to scan, it is useful to average many of the spectra. In this experiment, an average of 2000 scans was taken in order to obtain a well-defined

spectrum. The DSA output a trace of the running average every 200 in order to minimize the time it took for the DSA to actually trace the spectrum on the screen. The overload rejection option was also turned on. If the DSA detected a signal that was too large for its input, the DSA rejected that signal sample when taking the averages. If the overload rejection option was not on, including overload signals biased the averaged spectrum.

The physical units of the frequency-domain signal calculated by the DSA are $[\frac{V^2_{rms}}{Hz}]$, which is the so-called power spectral density. The Hanning window was selected. The Hanning window accepted the frequency spectrum in each frequency bin as a triangular window, i.e., the middle of the bin is weighted more heavily while the other points inside the bin are weighted less as a decreasing linear function. Calibrations of the DSA were also carried immediately before each spectral noise measurement. Further DSA setting options can be found in the operator's guide [12].

II.3. Noise Cancellation Techniques

Ambient electromagnetic noise was minimized so that the circuit wouldn't pick up extraneous noise. Because the resistor noise level is incredibly low, these measurements were incredibly sensitive. Any external electromagnetic noise could affect the measurements.

First, the circuit was placed inside a grounded metal box, as shown in **Figure 2-2.b**.

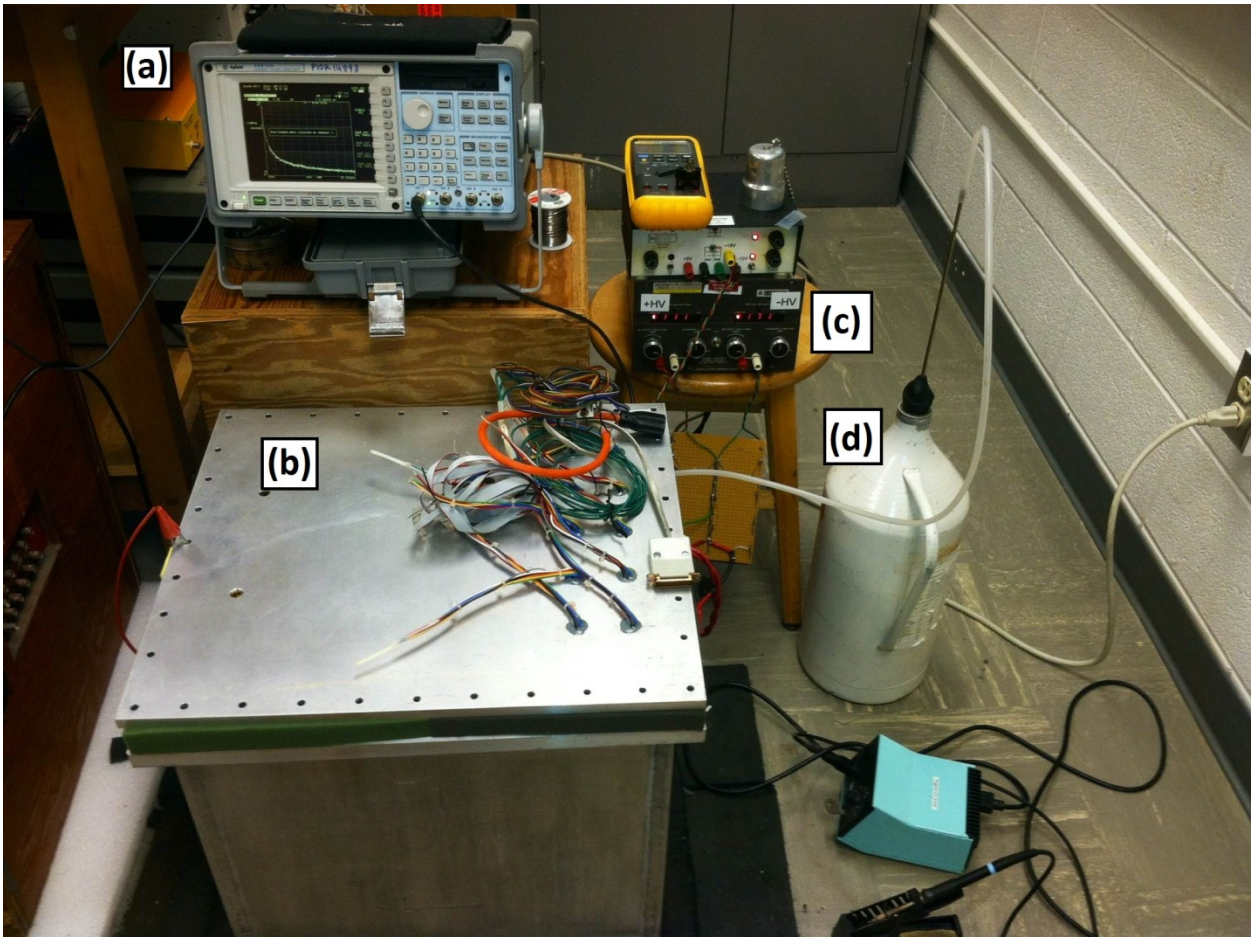

Figure 2-2: *A photograph of the experimental setup. (a) The Agilent 35670A Dynamic Signal Analyzer; (b) Metal box that the circuit is placed in to eliminate outside electromagnetic noise; (c) High voltage power supplies; (d) Dewar filled with liquid nitrogen to pull out humidity.*

The grounded metal box shields the circuit from any ambient electromagnetic waves (radio, TV, cell phones, ac power, etc.). Since metals are good conductors, the electromagnetic wave will travel on the top (or outside) of the box. Eventually, the waves will go to ground via the red clip on the left side of the box in **Figure 2-2**. This ground on the box is connected to the ground from the power supplies. In fact, any ground that is used in the system is associated with the power supplies' ground. That way, there is constant ground throughout the system, a technique called star-grounding.

All the cables used, viz., the power cables, the high voltage cables, and the grounding cables were twisted together so as to decrease the overall cross sectional area. An induced emf can be produced from a time-varying magnetic flux through the physical area enclosed by the cables. The induced emf has the formula:

$$\mathcal{E}(t) = -\frac{d\Phi_M}{dt} = -\frac{d\vec{B}(t)}{dt} \cdot \vec{A} \qquad \textbf{(Eq. 2-4)}$$

where Φ_M is the magnetic flux, $\vec{B}$ is the ambient magnetic field, and $\vec{A}$ is the physical area enclosed by grounded cables. Since $\frac{d\vec{B}(t)}{dt}$ cannot be controlled, $\mathcal{E}(t)$ is minimized by minimizing $\vec{A}$. If the cables were separated by a large open space, a large area would create a large induced emf. The power supply

cables and the DSA cables were plugged into the same outlet, and the cables were cable tied together to minimize the open area between them. The other cables were also cable tied to minimize the area between them. Also, the ac signal cables used in the experiment were coaxial cables, which screen out ambient electric fields.

In addition to the metal box and minimized cross-sectional area of the cables, a 4th-order RC filter was used on the power supply (item (c) in **Figure 2-2**). A 4th-order RC pi filter was constructed. An example of a 1st order RC pi filter is shown in **Figure 2-3**. The purpose of this filter was to eliminate 60-Hz harmonics caused by residual 60-Hz ac ripple in the ± HV dc power supplies. Since the ac wall power is at 60 Hz, spikes in the noise spectrum occur at harmonics of 60 Hz. As in the same way that the high-pass filter worked inside the circuit, the RC pi filter attenuated the 60-Hz harmonics. These spikes interfered with the data, and so the 4th-order RC pi filter was implemented, dramatically suppressing all 60-Hz harmonics. For this experiment, the RC pi filter had an RC time constant of 0.1 s associated with a 1-kΩ resistor and a 60-100-μF capacitor for each order. The frequency at −3 dB corresponding with the time constant is 1.6 Hz. The filter response at this frequency is 0.707, whereas at higher frequencies, the drop-off is 10 dB per decade of frequency. Therefore, at 60 Hz, the 4th-order RC pi filter gives a 40-dB rejection (i.e. a signal 10,000 times smaller).

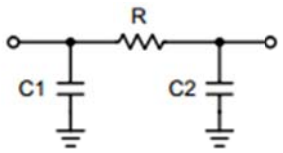

Figure 2-3: *A common RC pi filter. In this experiment, a 4th order RC pi filter was used. Figure courtesy of [13].*

II.4. Nitrogen Inerting

The metal box, which housed the circuit, was nitrogen inerted to rid the resistor under test of moisture. Carbon composition resistors are affected by humidity. It has long been known that CC resistors are hydroscopic, and readily absorb moisture when immersed in humid air. When the environment is humid, water molecules diffuse through the porous bakelite outer shell of the resistor and into carbon-clay conducting matrix of the CC resistor, which takes time. Since water is a conductive molecule, the transfer of current inside the resistor is affected by the presence of absorbed moisture.

As shown in **Figure 2-2.d**, the dewar is filled with liquid nitrogen. The evaporated nitrogen gas travels through the tube shown in **Figure 2-2** and dissipates into the metal box. Since the evaporated nitrogen is bone dry, the moisture in the resistors is evaporated out. This process takes some time, as the nitrogen had to diffuse throughout the environment, and the removal of water molecules from the resistors is also a diffusion process. Typical ambient relative humidity during the summer months over which resistor spectral noise data taken in the lab was RH ≈ 65%, which changed with daily weather patterns. The relative humidity, pressure, and temperature of the week of 8/19-8/26 in 2014 are shown in **Figure 2-4**. Measurements were taken using the Extech RHT50.

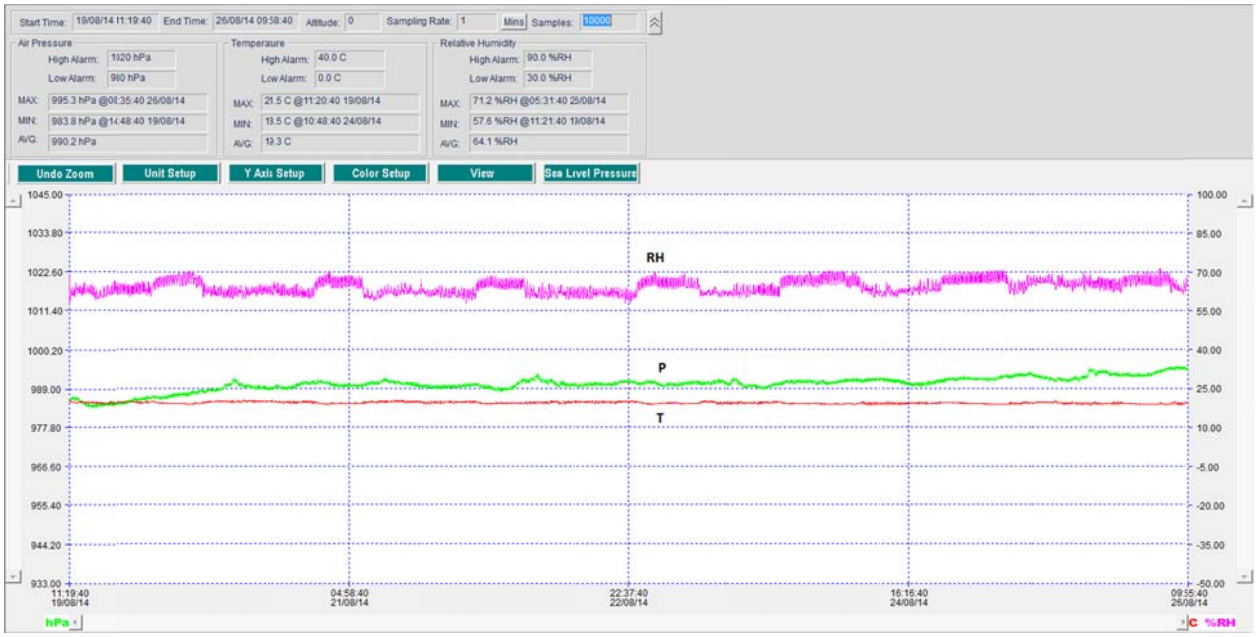

***Figure 2-4**: Measurements of relative humidity (RH) in pink, pressure (P) in green, and temperature (T) in red vs. time of the week. Pressure is measured in hPa on the left axis, RH is measured in percentage on the right axis, and T is measured in °C on the right axis.*

II.5. Taking the measurements

Different dc voltages were applied to the resistor under test. The high voltage power supplies were adjusted so that the positive and negative output voltages had approximately the same magnitude. A picture of the cables into the circuit is shown in **Figure 2-5**. The positive and negative voltages were changed by the knobs on the HV power supply (see **Figure 2-2.c**). The output voltage from the power supply was set by measuring the voltage across the resistor under test using a Fluke 87 digital multi meter. The noise spectrum was taken at a fixed voltage across the resistor. These voltages were: 15.00 V, 30.00 V, 50.0 V, 70.0 V, 90.0 V, and 110.0 V.

The noise floor for each of the resistors was also measured. The HV power supply is turned off for this measurement. This noise floor was subtracted from the noise spectra at each dc voltage across the resistor. The resulting noise spectra represented the true noise spectra for each dc voltage across the resistor.

Before taking any measurements, a 20-minute waiting period was enforced to let the resistor thermally equilibrate at its dc voltage. Because electrical power, $P = VI = V^2/R$ (watts) is dissipated through a resistor as heat, it was important for the resistor to reach thermal equilibrium with itself. A solid-state TMP35 temperature sensor was placed on the resistor under test. The temperature was monitored until it reached a stable temperature. After 20 minutes, the temperature was observed to remain constant. Thermal equilibrium was assumed to be reached at that time. Twenty minutes after the dc voltage was applied to each resistor, the DSA began recording spectral noise measurements. At least three measurements were taken for the applied dc voltage for each resistor to assess the reproducibility and stability of the measurement.

The resistors under test were connected to the circuit to measure the spectral noise of different resistors. As can be seen in **Figure 2-6**, the arrow points to the resistor under test. This resistor is connected to the noise measuring circuit by soldering the resistor leads to the MF resistors.

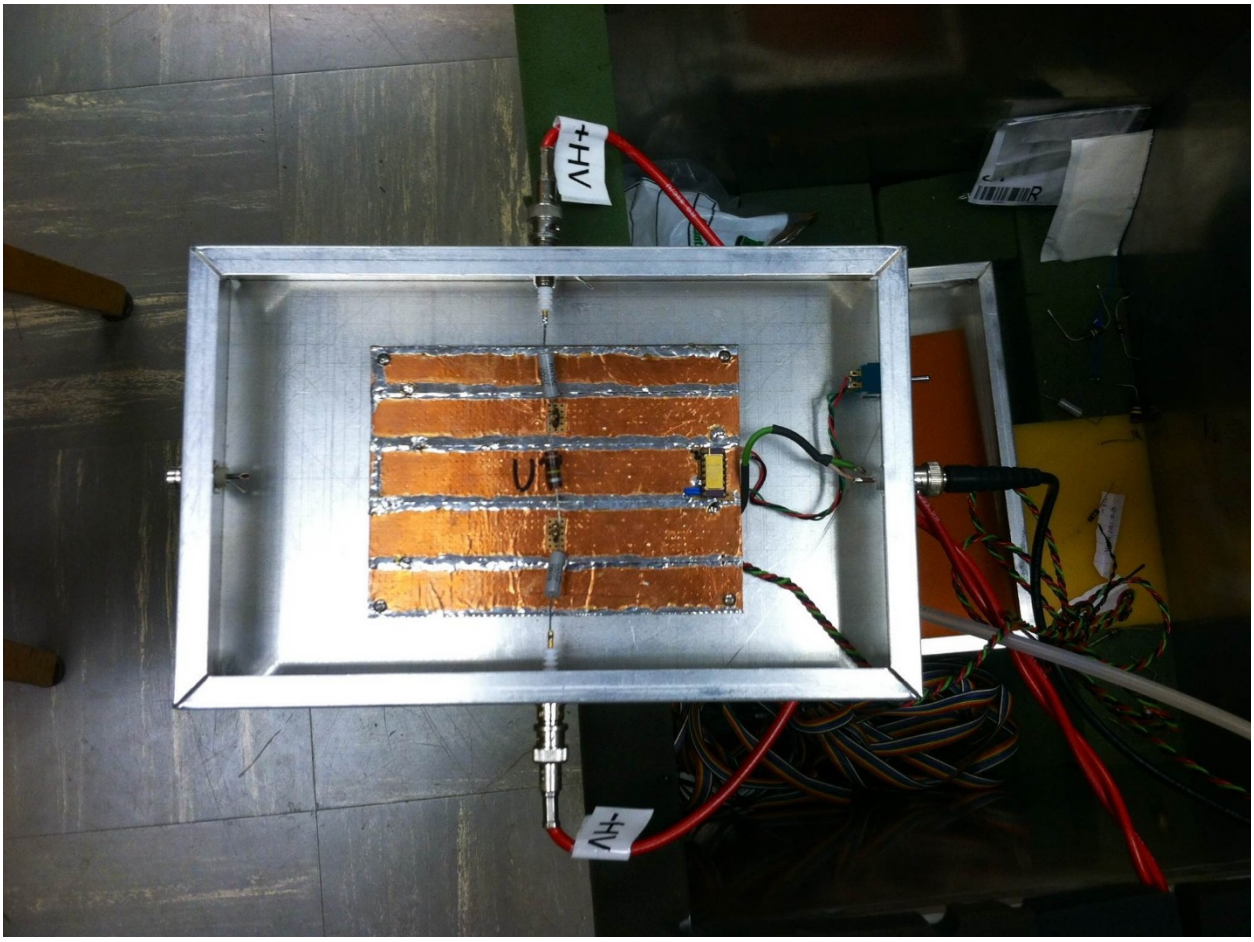

Figure 2-5: *A photograph of the test circuit. The positive and negative voltages come through the red cables labeled "+HV" and "–HV", respectively. The chip to the far right of the circuit board circled in red is the AD624. The output of the circuit is through the black cable located at the far right center of the box indicated by the blue arrow.*

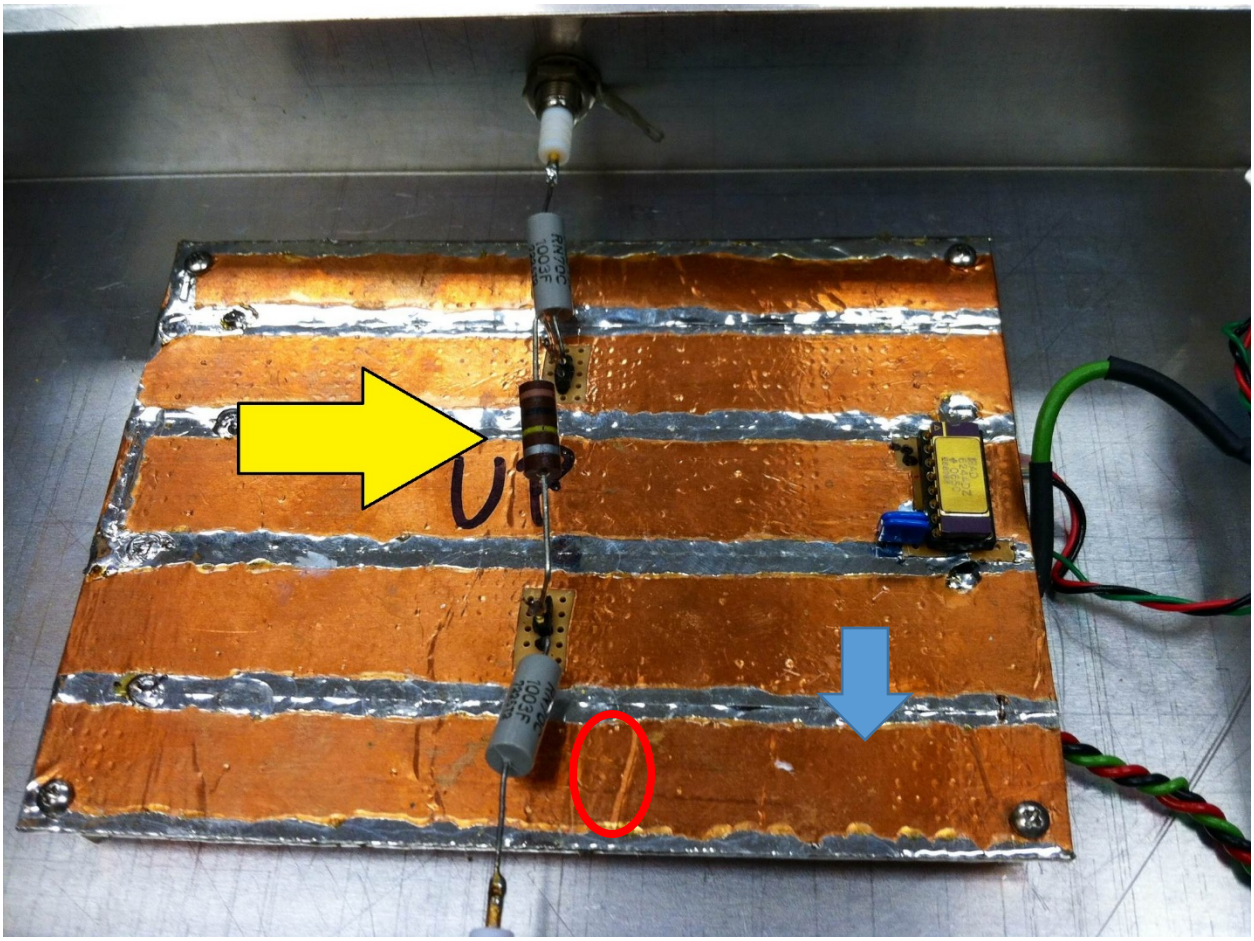

Figure 2-6: *A close up of the circuit board. The arrow points to the device under test (DUT). In this figure, the DUT is a 100 kΩ 1-W CC New Stock (NS) resistor. The grey resistors are 100-kΩ 1-W MF resistors.*

The resistor noise spectrum was then taken by the DSA. The spectral noise data files were read into the computer via USB using the DataLink software provided by Agilent. These files were then converted to text files, and the text files were then read into MATLAB data analysis scripts. The MATLAB coding framework was used for analysis of the data through plots and least-squares fits to the spectral noise data.

III. Results

III.1. The Absolute Noise Floor of the DSA

In order to understand the totality of the noise of the circuit, the noise floor for the DSA must be first taken into account, although all of the different noise sources in the circuit must also be accounted for. The DSA provides the absolute lowest noise signal that can be measured. The dominant contributor to the noise spectrum will be the DSA only when the noise levels are low enough.

A 50-Ω terminator was used on the DSA input to simulate the low output impedance of the AD624 instrumentation op-amp. The AD624 has an output impedance of ≈ 50 Ω [10], so the terminator

also acts as the value for the output impedance of the AD624. The 50-Ω terminator also screens out any ambient electromagnetic signal before it enters the BNC input of the DSA.

The 50-Ω terminator also has its own thermal noise to consider, namely $S_{V^2}(f) = 4k_B T R_{50\Omega} = 8.0633 \times 10^{-19}\ [\frac{V_{RMS}^2}{Hz}]$. However, the level of the 50-Ω thermal noise is negligible in this case, as it contributes a very small amount to the overall noise of the DSA.

At around 4.5×10^{-16} V^2_{rms}/Hz, the absolute noise floor of the DSA must be the smallest, combined source of noise in the circuit. Nothing for the $1/f$ spectral noise measurements can be smaller than the noise floor associated with the DSA.

The noise floor of the DSA with a 50-Ω terminator connected to its input is shown in **Figure 3-1**.

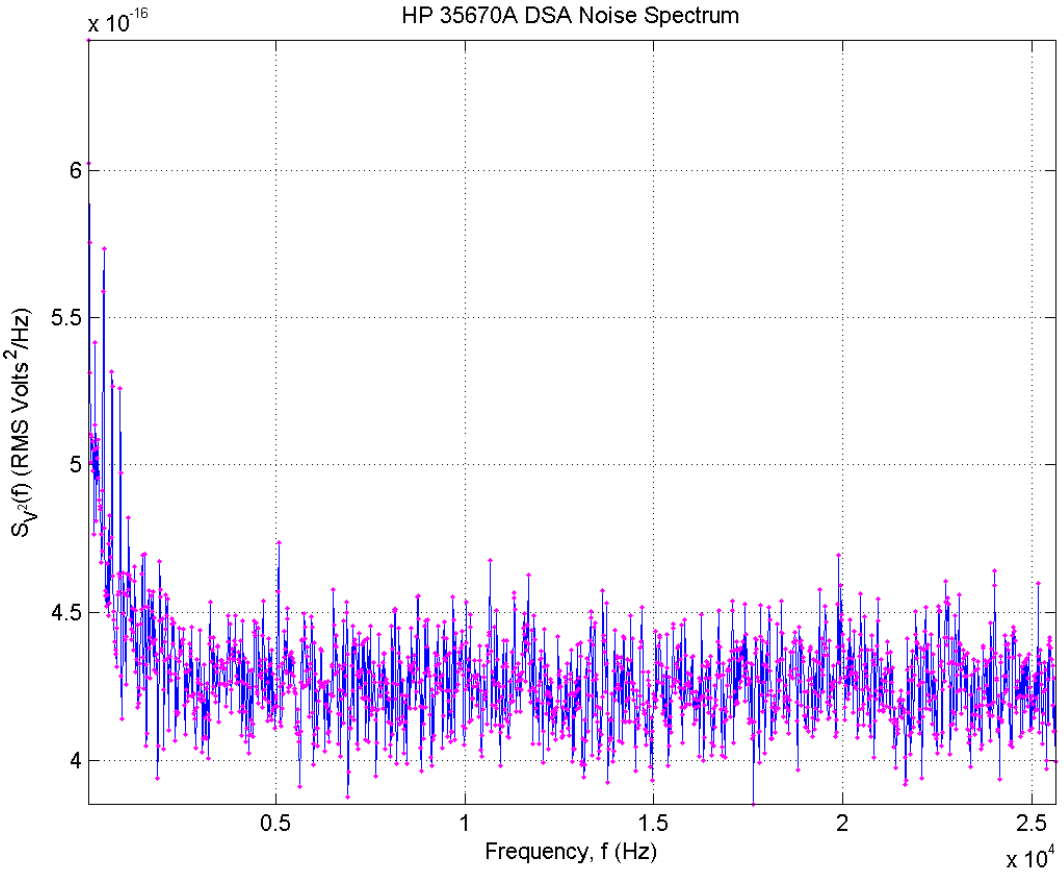

Figure 3-1*: The noise floor of the DSA with the 50-Ω terminator connected to its input. The signal remains relatively flat for most of the spectrum (from 2.5 kHz onwards).*

The shape of this noise floor is relatively flat, i.e., the noise floor has little frequency dependence on it. Except for the small frequency dependence at the beginning of the frequency spectrum, the noise remains relatively flat (refer to the *y*-scale in **Figure 3-1**.)

III.2. The noise floor for the resistors with HV off

Taking the noise floor spectrum for each resistor with high voltage off shows the total noise for the high-voltage independence of that configuration. By subtracting the HV-off spectrum from the HV-on spectrum, all non-1/*f*-noise (HV independent) contributions are removed.

The noise floor for the 100-kΩ 1-W MF resistor shows the general lack of frequency-dependent noise of the circuit. **Figure 3-2** shows the noise floor for the metal film resistor.

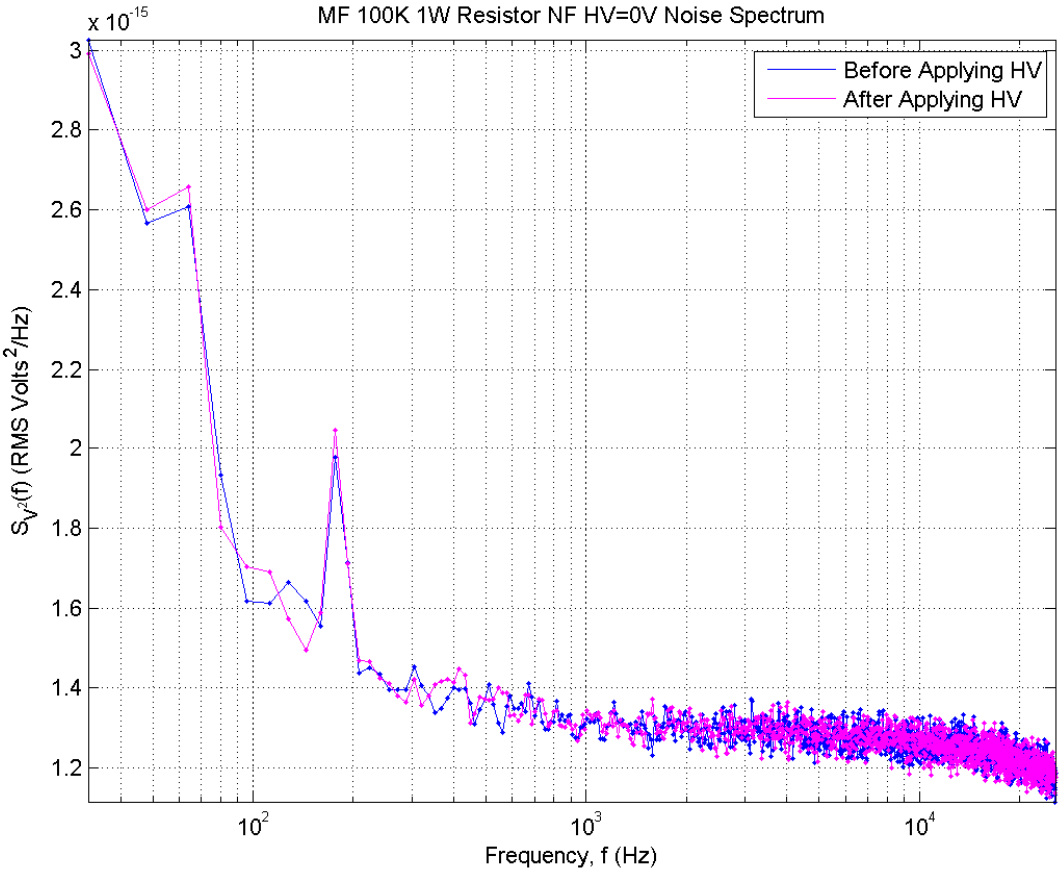

***Figure 3-2**: The HV off noise floor for the 100-kΩ 1-W MF resistor. Here, the two curves were taken before and after applying the high voltages to the resistor. The difference is negligible. These data are raw and do not have the DSA noise floor subtracted.*

Here, the HV noise floor is generally flat. In the same way the DSA noise floor had more noise at the lowest end of the spectrum, the MF noise floor agrees. A roll-off occurs at the highest frequencies; a discussion of this phenomenon is given in **Appendix 1**.

These spectral data are representative of the metal film resistors used elsewhere in the circuit as well. Since they have no significant frequency dependence on noise, the metal film resistors, and the circuit in general, has no significant frequency dependence on noise. Thus, when measuring resistor 1/*f* noise, the strong frequency dependence will be obviously from the resistor under test.

The carbon composition resistors have a voltage dependence on their 1/*f* noise, so the HV off noise floor shows the zero-voltage component for each carbon composition resistor. Each resistor has the same amount of thermal noise because all resistors had the same resistance (100 kΩ). Since the 1/*f* noise is high-voltage dependent, the noise floors for each resistor should look relatively the same. The thermal noise of the circuit should be the same regardless of which resistor is present.

Figure 3-3 depicts the noise floor for the 100-kΩ 1-W high-reliability (Hi-Rel) CC OS resistor. Here, the noise floor is measured with the high-voltage power supply off and on, but set to a minimum.

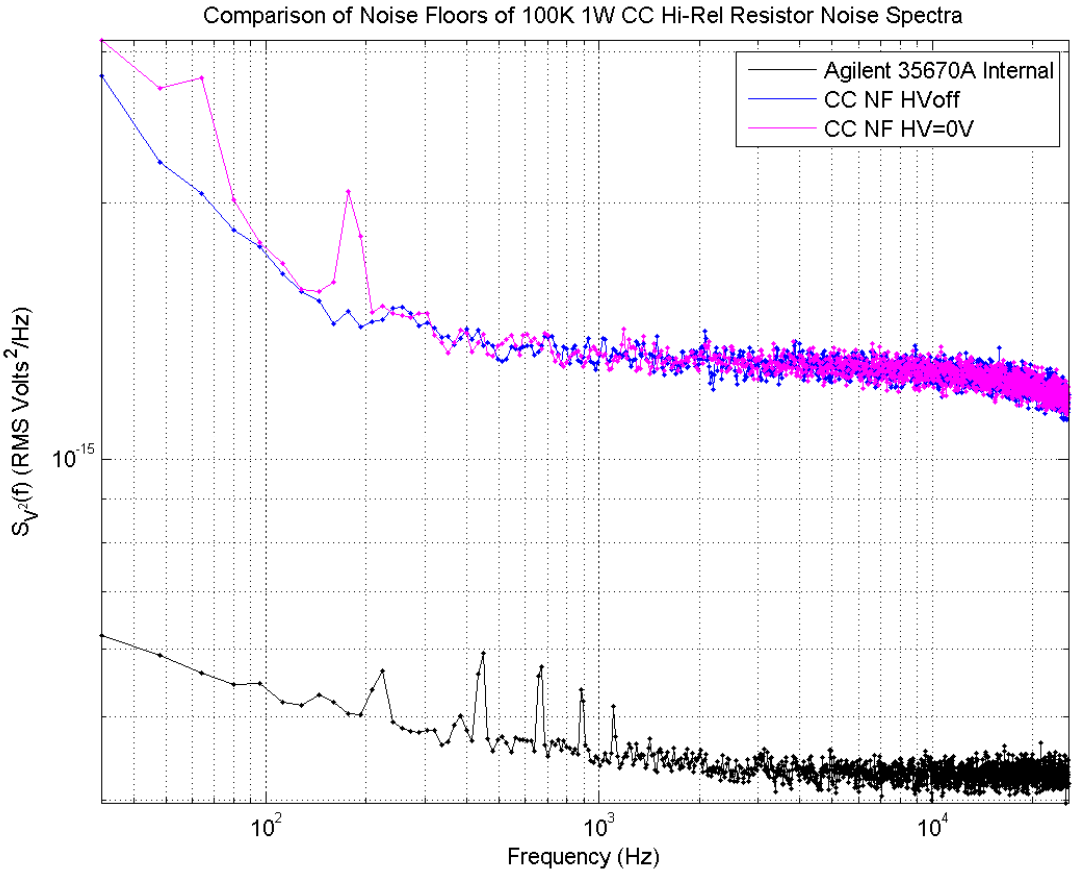

***Figure 3-3**: These data show the 100-kΩ 1-W Hi-Rel CC OS resistor noise floors. A large gap exists between the noise floor of the DSA and for the resistor. The difference between the high-voltage power supply being off and being on at a minimum seems to be negligible except at low frequencies*

The other CC resistors behave in a manner similar to that of the resistor shown in **Figure 3-3**.

The TF resistor, like the others, has a generally flat noise floor over the spectrum, allowing subtraction of this noise floor for the high-voltage data. The spectral noise floor of the TF resistor before and after applying high voltages is shown in **Figure 3-4**.

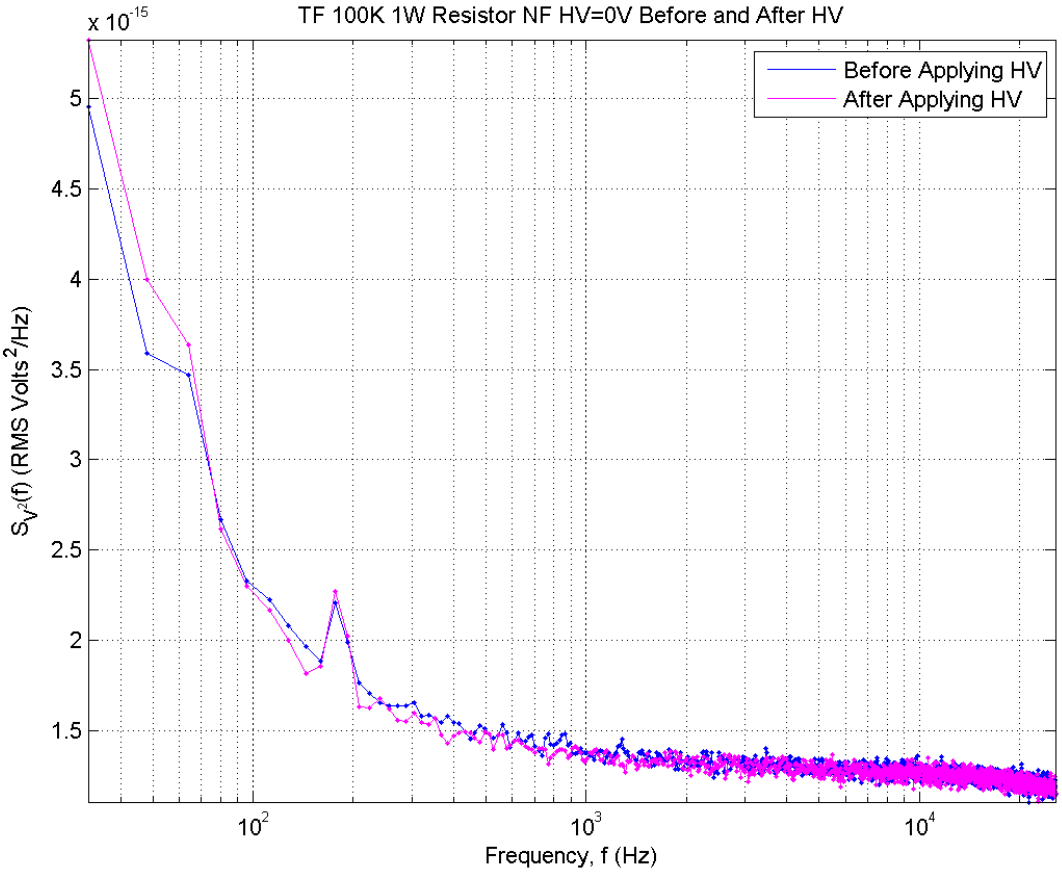

***Figure 3-4**: The noise floor for the 100K 1-W TF resistor. Again, the difference between the high voltage on and set to a minimum is negligible except at low frequencies.*

A plot showing the noise floors of the DSA along with all of the resistors is shown in **Figure 3-5**. NB, the high voltage power supply is not turned on for these measurements.

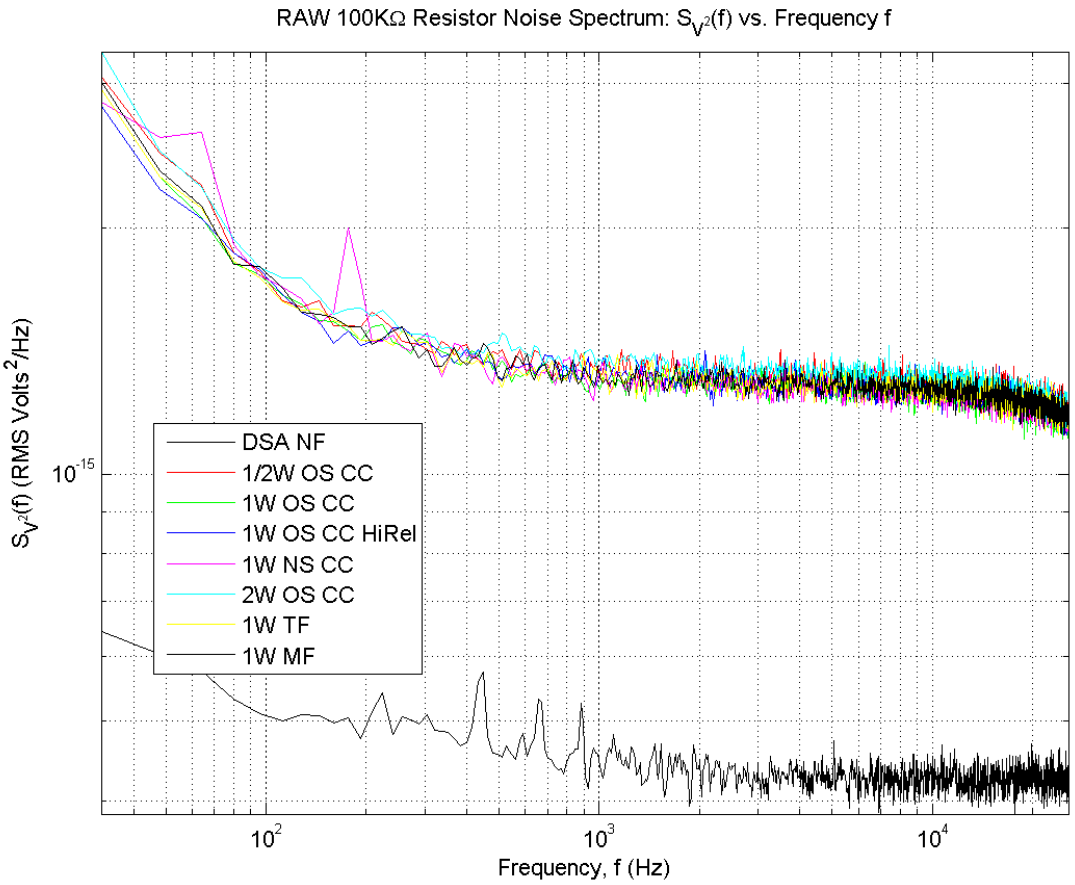

***Figure 3-5**: The noise floors of the DSA as well as the resistors as shown. The low frequency noise is higher than the rest of the flat spectrum. Also, the spike associated with the 1/2-W noise floor data is associated with the 60-Hz harmonics from the ac line voltage.*

The tail from the high frequency spectrum is associated with the stray input capacitance from the AD624. More discussion of this phenomenon is in **Appendix 1**.

III.3. Time Stability for each resistor

Each resistor was tested for multiple runs even after waiting for 20 minutes to thermally equilibrate the resistor. To visually see the precision of the noise spectrum, a scan was made multiple times for each resistor at each high voltage.

Some of the resistors took a short time to fully equilibrate, such as the MF and TF resistors. **Figure 3-6** shows the time stability wait for the 100-kΩ 1-W TF resistor.

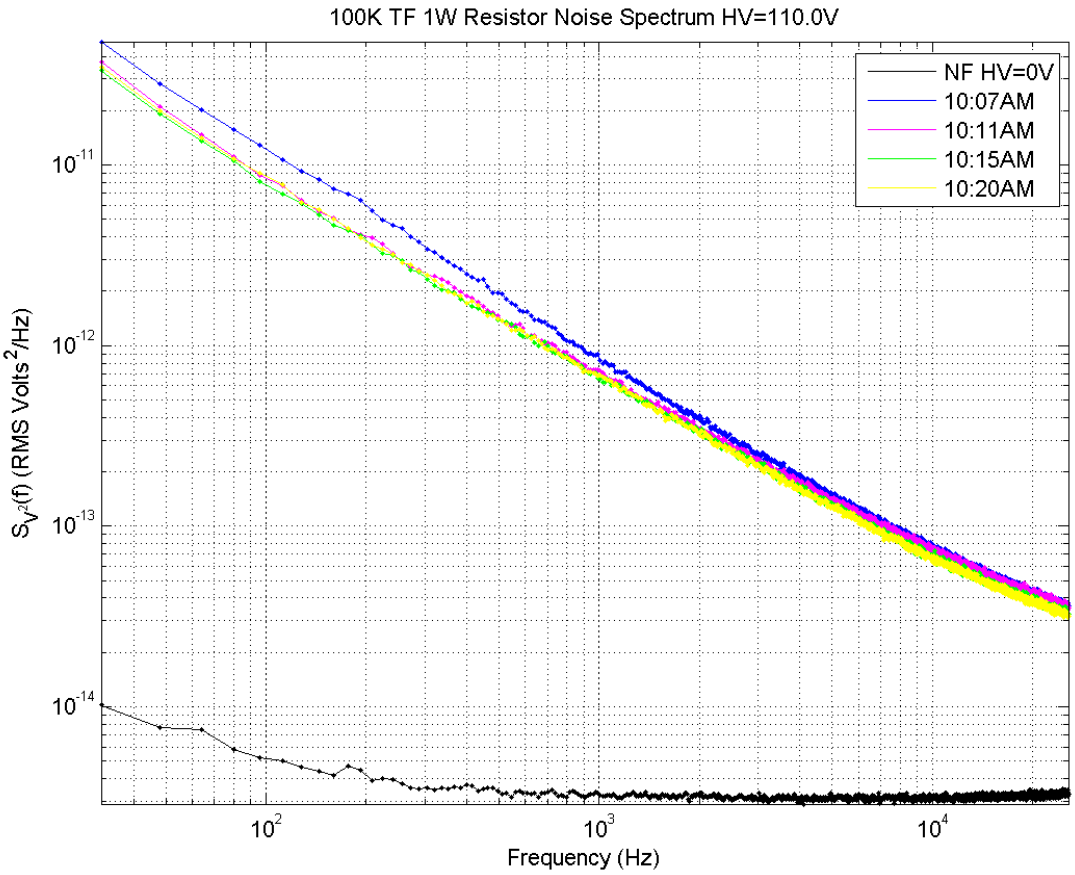

***Figure 3-6**: The time stability plot for the TF resistor at 110.0 V. There was 20 minutes before the voltages were turned on. The first measurement is at 10:07AM, where it is noticeably not consistent with the rest of the curves. The overall stability time was roughly 13 minutes after the 20 minutes of thermal equilibration.*

The MF resistor also does not take long to stabilize. The construction of the MF and TF resistors is different from the CC resistors.

The CC resistors took much longer to fully equilibrate for any power rating. **Figure 3-7** shows a time stability plot for the 100-kΩ 2-W OS CC resistor. Here, the noise spectrum for this resistor starts out unstable. However, after some time, the resistor equilibrates and the noise spectrum becomes stable.

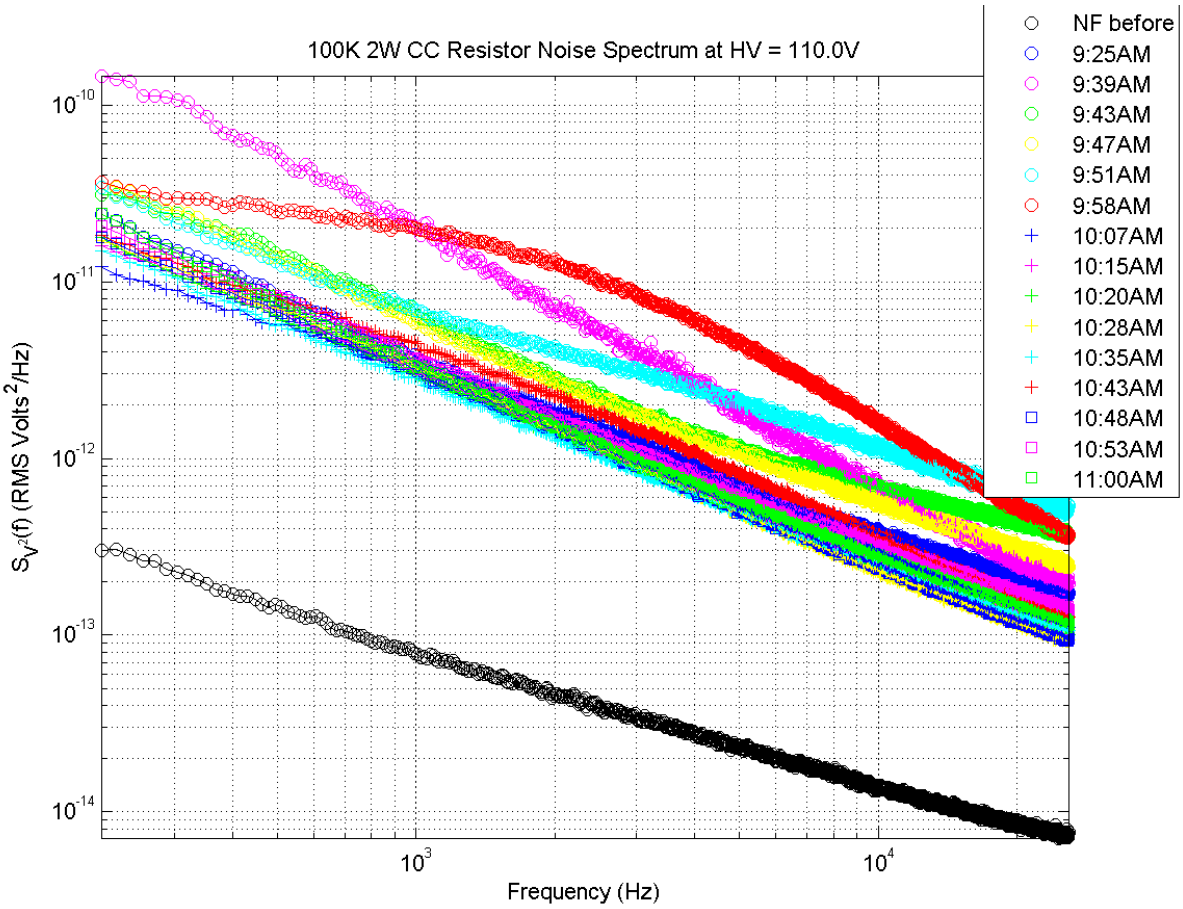

***Figure 3-7**: A plot of the noise spectrum for the 100-kΩ 2-W CC OS resistor at 110 V. The noise spectrum is unsteady shortly after waiting 20 minutes for thermal equilibrium. After about an hour and a half, the spectrum was stable.*

The other CC resistors did not have as long of a wait time as the 2-W CC resistor, but the wait to stabilize was longer in the CC resistors than in either the TF or MF resistors. The wait was generally less as the time the resistor had been exposed to high voltage went on.

III.4. Noise spectra for each resistor vs HV

The primary goal of the experiment was to measure the 1/*f* noise in carbon composition and thick film resistors, and the results in the following subsections present these results.

Metal Film 100-kΩ Resistor

The metal film resistor was not expected to produce 1/*f* noise. The main contributor of the noise from the 100-kΩ MF resistor was thought to be Johnson-Nyquist noise. **Figure 3-8** below shows the noise floor subtracted spectrum results for the 100-kΩ MF resistor.

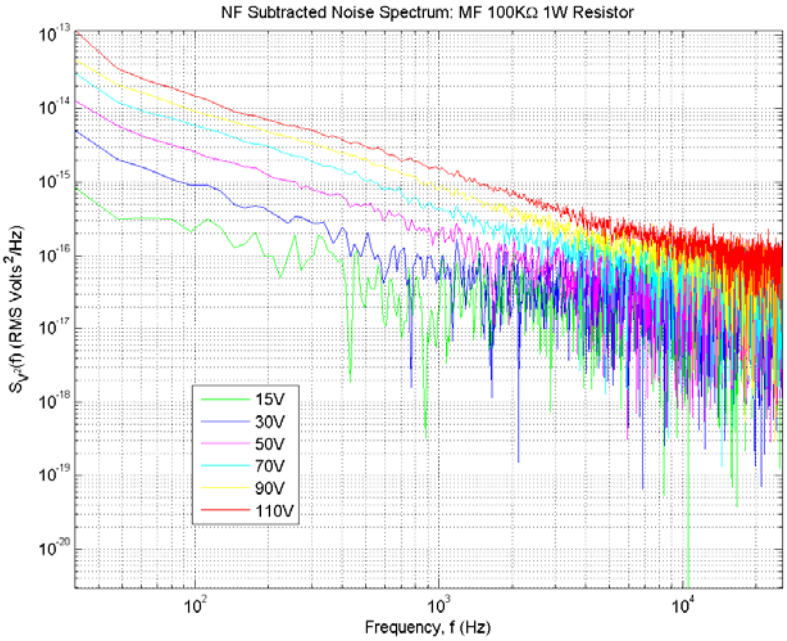

***Figure 3-8**: The noise floor subtracted spectrum for the MF 100-kΩ resistor. The spectrum shows 1/f noise at low levels.*

Thick Film 100-kΩ Resistor

The TF resistor was expected to exhibit 1/*f* noise. **Figure 3-9** below shows the noise floor subtracted spectrum for the 100-kΩ 1-W TF resistor.

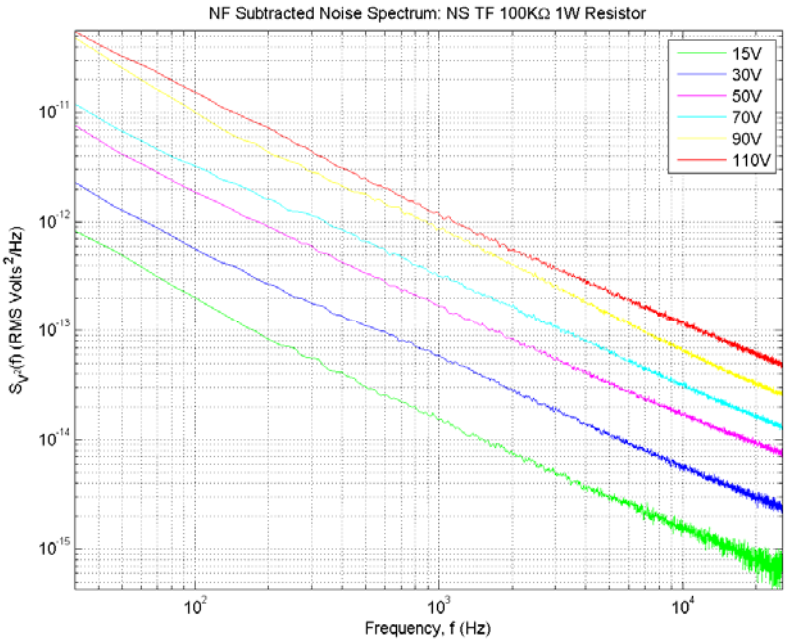

***Figure 3-9**: The noise floor subtracted spectrum for the TF 100-kΩ resistor. The spectrum shows 1/f noise.*

1-W Old Stock High-Reliability Carbon Composition 100-kΩ Resistor

The 1-W OS Hi-Rel CC 100-kΩ resistor was expected to exhibit 1/*f* noise. **Figure 3-10** below shows the noise floor subtracted spectrum for the 100 kΩ 1-W OS Hi-Rel CC resistor.

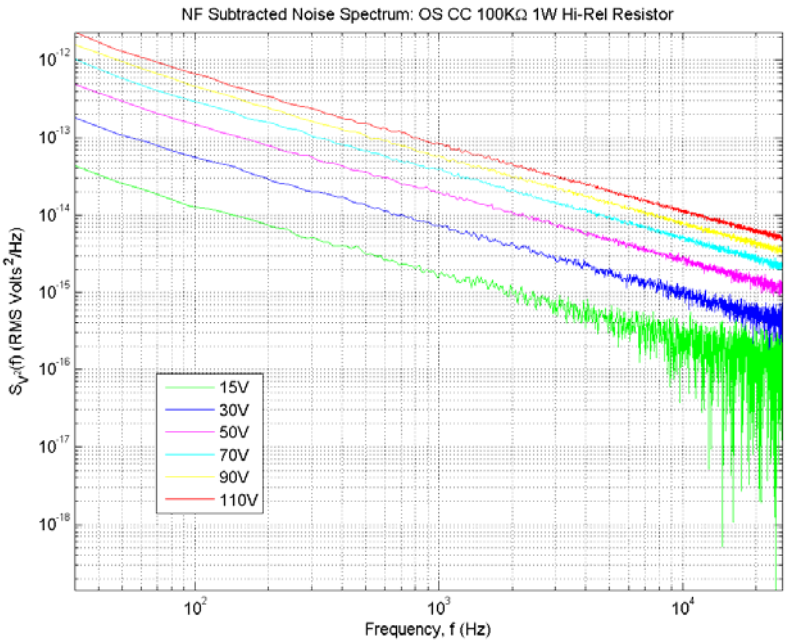

***Figure 3-10**: The noise floor subtracted spectrum for the 1-W OS Hi-Rel 100-kΩ CC resistor. The spectrum shows 1/f noise.*

½-W Old Stock Carbon Composition 100-kΩ Resistor

The ½-W OS CC 100-kΩ resistor was expected to exhibit 1/*f* noise. **Figure 3-11** shows the noise floor subtracted spectrum for the 100-kΩ 1/2-W OS CC resistor.

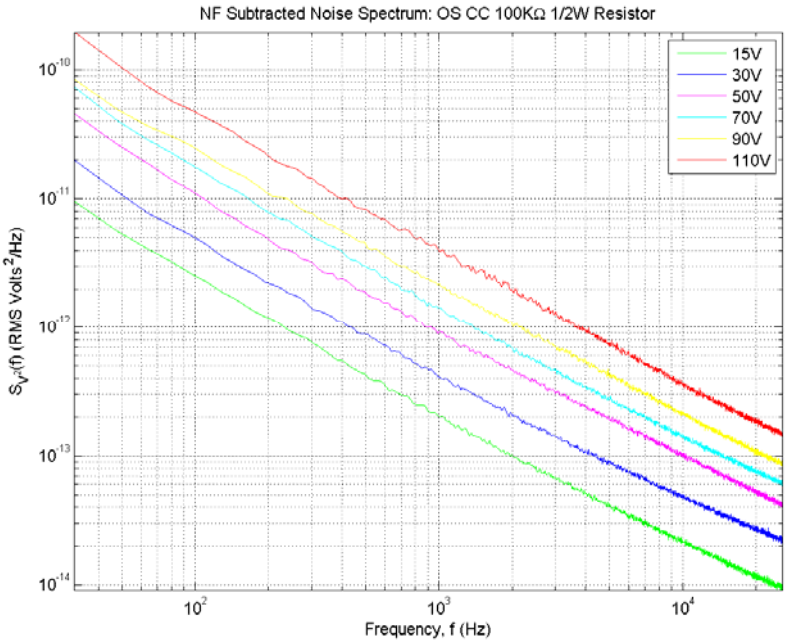

***Figure 3-11**: The noise floor subtracted spectrum for the 1/2-W OS CC 100-kΩ resistor. The spectrum shows 1/f noise.*

1-W Old Stock Carbon Composition 100-kΩ Resistor

The 1-W OS 100-kΩ CC resistor was expected to exhibit 1/*f* noise. **Figure 3-12** below shows the noise floor subtracted spectrum for the 100 kΩ 1-W OS CC resistor.

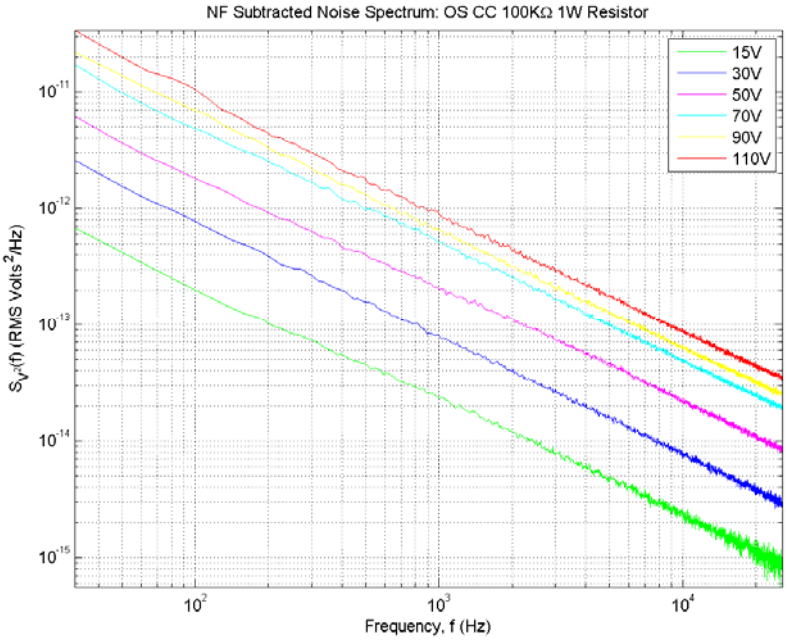

***Figure 3-12**: The noise floor subtracted spectrum for the 1-W OS CC 100-kΩ resistor. The spectrum shows 1/f noise.*

2-W Old Stock Carbon Composition 100-kΩ Resistor

The 1-W OS CC 100-kΩ resistor was expected to exhibit 1/*f* noise. **Figure 3-13** below shows the noise floor subtracted spectrum for the 100-kΩ 2-W OS CC resistor.

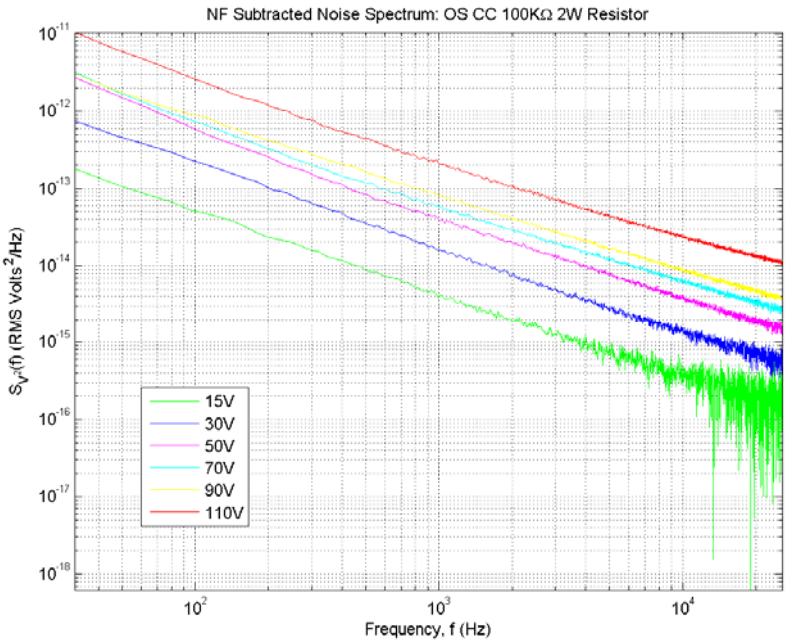

***Figure 3-13**: The noise floor subtracted spectrum for the 2-W OS CC 100-kΩ resistor. The spectrum shows 1/f noise.*

1-W New Stock Carbon Composition 100-kΩ Resistor

The 1-W NS CC 100-kΩ resistor was expected to not exhibit perfect 1/*f* noise. **Figure 3-14** shows the noise floor subtracted spectrum having the noise floor subtracted for the 100 kΩ 1-W NS CC resistor.

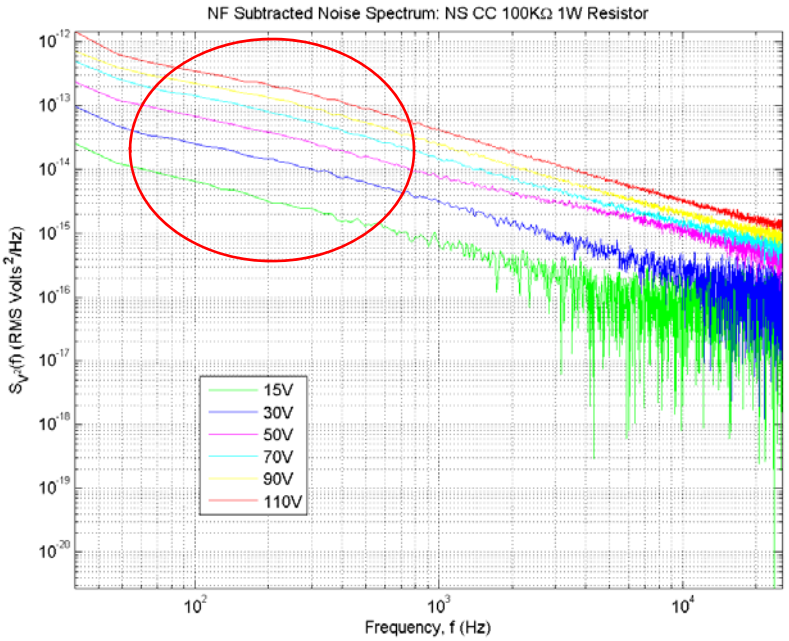

***Figure 3-14**: The noise floor subtracted spectrum for the 1-W NS CC 100-kΩ resistor. The spectrum shows departures from 1/f noise spectra. The red circle in the plot shows the deviation from 1/f.*

III.5. Humidity effect

As described in the **Methods** section, the RH of the lab had to be removed from the resistor. Moisture inside the resistor adds to the spectral noise, in an uncontrollable (by us) time-dependent manner. The ½-W CC resistor's 1/*f* noise spectrum was measured after having been exposed for several days to the humid environment. A comparison between the noise at 90.0 V_{dc} of the bone dry resistor and the resistor exposed to humidity is shown in **Figure 3-15**. The noise floor has been subtracted from both spectra. Interestingly, the resistor with nitrogen inerting exhibits a significantly higher 1/*f* spectral noise level.

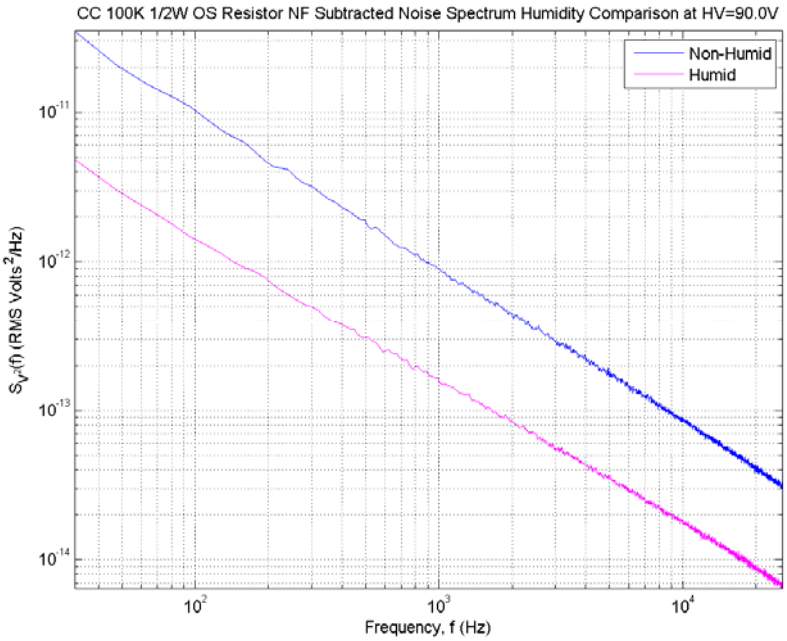

***Figure 3-15**: Comparison of the noise spectra at 90 V_{dc} of the 1/2-W OS CC 100-kΩ resistor being exposed to a humid environment and being nitrogen inerted. The nitrogen-inerted resistor shows higher levels of 1/f noise.*

III.6. Universal scaling

For each resistor, the six parallel 1/*f* noise spectra are related to each other by a universal scaling factor. By dividing the noise spectrum by the high voltage across it raised to some power, γ, the six curves all line up with each other, as shown in **Figure 3-16**.

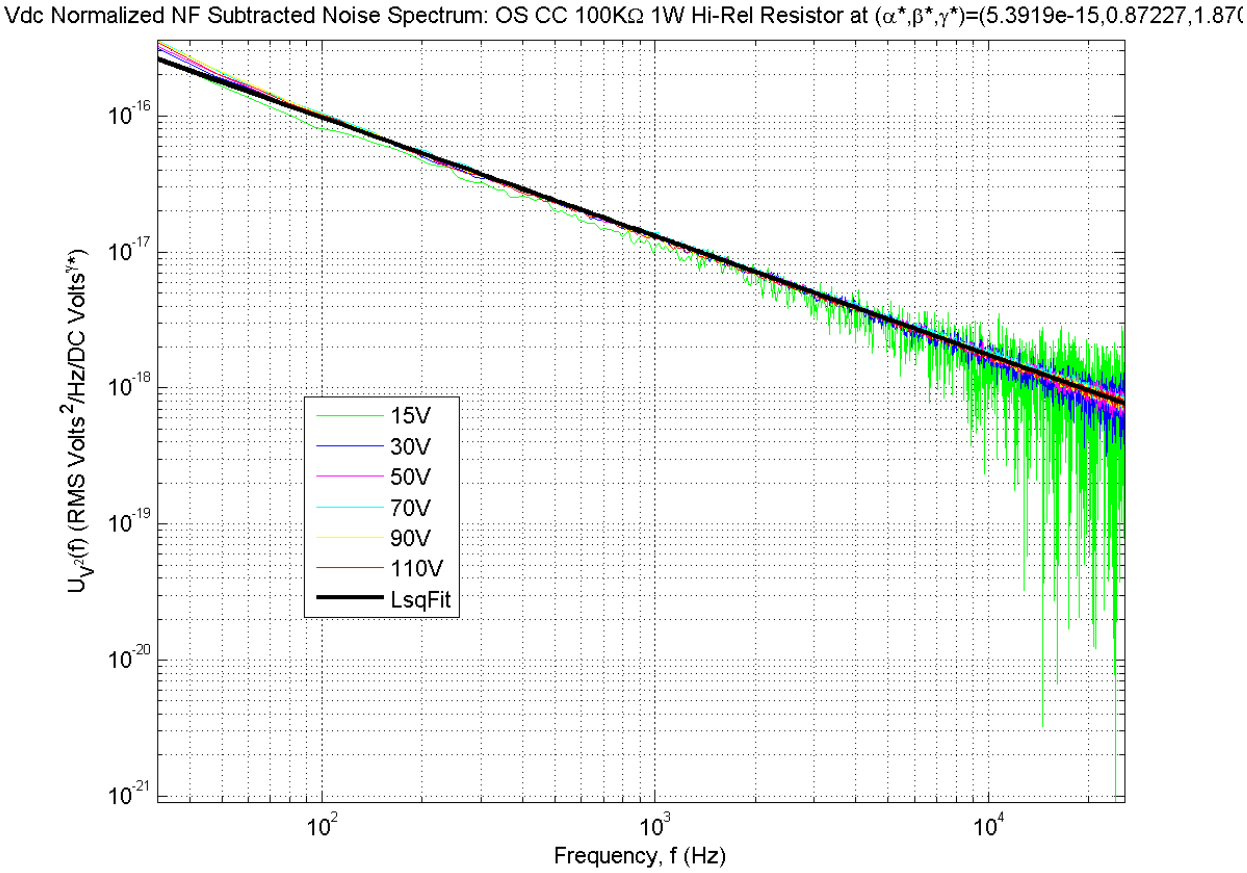

***Figure 3-16**: The normalized noise floor subtracted noise spectra of the 1-W Hi-rel CC 100k resistor. The six HV curves are normalized and line up with each other.*

Each individual measurement makes a plane in 3D, as can be seen in **Figure 3-17**.

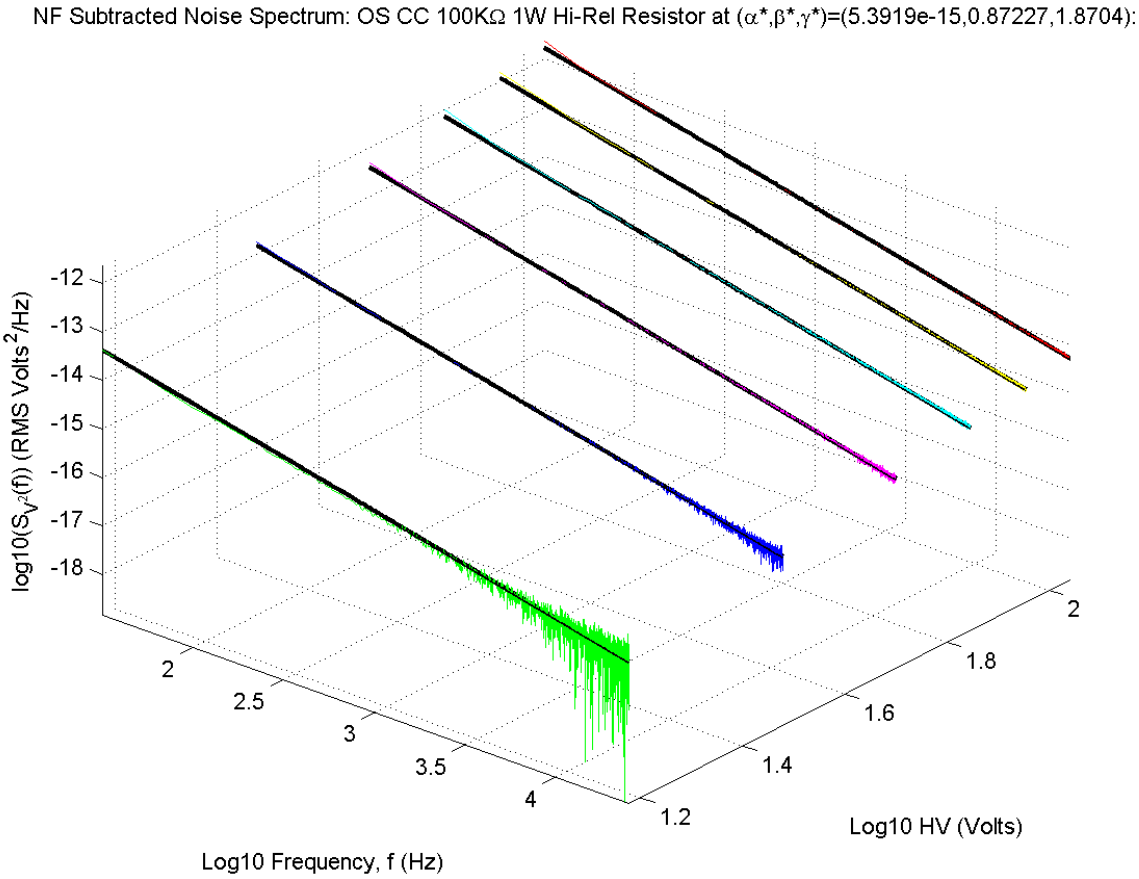

***Figure 3-17**: A 3D representation of the noise spectrum for the OS CC Hi-Rel resistor as function of high voltage. The curves make up a plane with slope along the HV axis, γ. The black lines represent the linear fit of each noise spectra.*

A new noise spectrum, one for each resistor, was calculated by the equation below:

$$U_{V^2}(f, V_{dc}) = \frac{S_{V^2}(f)}{V_{dc}^{\gamma}} \quad [\frac{V_{rms}^2}{Hz}] \qquad \textbf{(Eq. 3-1)}$$

where $U_{V^2}(f, V_{dc})$ is the universal scaling equation, $S_{V^2}(f)$ is the measured noise spectrum from the DSA, V_{dc} is the dc voltage applied across the resistor under test, and γ is the universal scaling parameter. More discussion on this equation will appear in the **Discussion** section.

Each resistor has its own value for the parameter, γ. In **Table 3-1**, the results for the γ values are listed, which are obtained from a 1-parameter least-squares fit to the six noise-floor subtracted $1/f$ noise spectra for each resistor.

***Table 3-1**: Gamma values for resistors*

Resistor Type	γ value
½-W OS CC	1.3700 ± 0.0004
1-W OS CC	1.8677 ± 0.0006
1-W OS Hi-Rel CC	1.8822 ± 0.0014
1-W NS CC	1.9024 ± 0.0021
2-W OS CC	1.8954 ± 0.0011
1-W NS TF	2.2248 ± 0.0007
1-W MF	1.8635 ± 0.0076

More discussion on the *γ* scaling factor will appear in the **Discussion** section.

IV. Discussion

IV.1. Thermal Noise

Any non-1/f noise produced by the resistor is much less than the 1/f noise when high voltage is applied. As can be seen by **Figure 3-5**, the HV off noise floor for all the resistors is close to $S_{V^2}(f) = 1.5 \times 10 - 15\ \mathrm{V}_{\mathrm{rms}}^2/\mathrm{Hz}$. This quantity actually follows very closely with the Johnson noise equation given by [14]:

$$S_{V^2}(f) = 4k_B TR \quad [\frac{V_{rms}^2}{Hz}] \qquad \textbf{(Eq. 4-1)}$$

Where k_B is Boltzmann's constant, *T* is the temperature, and *R* is the resistance. Since these values are all assumed to be the same (*T* ≈ 292.15 K, *R* = 100 kΩ), the noise floor being the same for all resistors makes sense.

Johnson-Nyquist noise is most important to take into account at high frequencies where the 1/*f* noise falls off in the spectra when high voltage is applied. At high frequencies, the 1/*f* noise falls off, and the flat Johnson-Nyquist noise dominates. An example of how this appears graphically is shown in **Figure 4-1**.

The frequency range of this experiment, however, does not examine extremely frequencies such that Johnson-Nyquist thermal noise dominates. The noise floor for these data must be subtracted, because the focus of the experiment is to measure the 1/*f* noise contributions of the resistors.

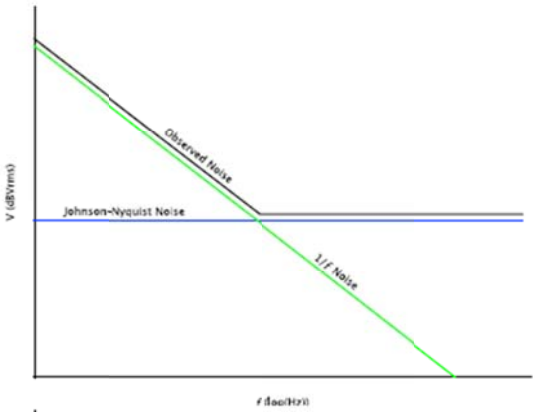

***Figure 4-1**: The 1/f noise produced falls linearly on a log-log plot, so the noise contribution for 1/f noise will be smaller than the Johnson-Nyquist noise at high frequencies. Image courtesy of [15].*

As can be seen in the noise floor spectra shown in **Figures 3-2** through **3-5**, the noise levels roll off at high frequencies. This effect is caused by a non-zero stray capacitance at the ± inputs of the AD624. Thermal noise spectral measurements were carried out up to 52.232 kHz as the roll off was greater at higher frequencies.

The stray capacitance was modeled as ideal capacitors connecting the ± inputs of the AD624 op-amp to ground. The stray capacitance was calculated through a MATLAB least squares fit program which swept values for the stray capacitance. This stray capacitance value was 60.6 pF ± 0.2 pF. A detailed circuit model including C_s, the stray capacitance, was then used to correct for the high frequency roll off so that the thermal noise measurements were flat across the frequency spectrum.

In addition, other resistors in the circuit load down the resistor under test, meaning each resistor has a transfer function associated with it. Each resistor is its own noise source for the total noise source of the circuit. By taking that into account, the level of noise associated with only the resistor under test was determined. The transfer function for the resistor under test accounts for 90.9% of the noise of the circuit. The results of the noise levels were corrected. Note that the inclusion of the transfer function has a large effect on the α parameter. More discussion on resistor thermal noise is given in **Appendix 1**.

IV.2. Shot Noise

Another type of noise that is not seen in the measurements is shot noise, whose theoretical formula is given in **Eq. 4-2**

$$I_{noise}(f) = \sqrt{2 I_b Q_e} \quad [\frac{Amps}{\sqrt{Hz}}] \qquad \textbf{(Eq. 4-2)}$$

where I_b is the dc bias current, and Q_e is the charge of an electron given by 1.6×10^{-19} C. To get the corresponding voltage noise, I_{noise} is first multiplied by the resistance by Ohm's law, then squared. For example, if HV were 100 V_{dc}, R is 100 kΩ, I_b is 1 mA. $I_{noise}(f) = \sqrt{2 * 10^{-3} * 1.6 \times 10^{-19}} = 1.79 \times 10^{-11} \frac{Amps_{rms}}{\sqrt{Hz}}$. Multiplying by 10^5 Ω and squaring gives $S_{V^2_{I_{noise}}}(f) = 3.2 \times 10^{-12}\ V^2_{rms}/Hz$. However, we do not observe this noise.

Shot noise is in fact not present inside macroscopic resistors. This noise is masked inside of the resistors due to strong phonon-electron interactions. Since the resistor is a macroscopic object with many charge carriers, shot noise is a negligible effect in any of the resistor noise measurements. Shot noise is important in systems with very short length scales such as transistors in integrated circuits. In fact, shot noise is present at a low level at the ± inputs of the AD624.

IV.3. Output Power and Current

Since the resistors under test produce some ac noise voltage, other quantities can be derived such as ac noise current and ac noise power. From basic electronics, the power, *P*, is given by $P = V^2/R$. In this experiment, V^2/Hz is measured. The output noise of the resistor divided by its resistance gives power in W_{rms}/Hz. An example of this calculation is shown in **Figure 4-2**.

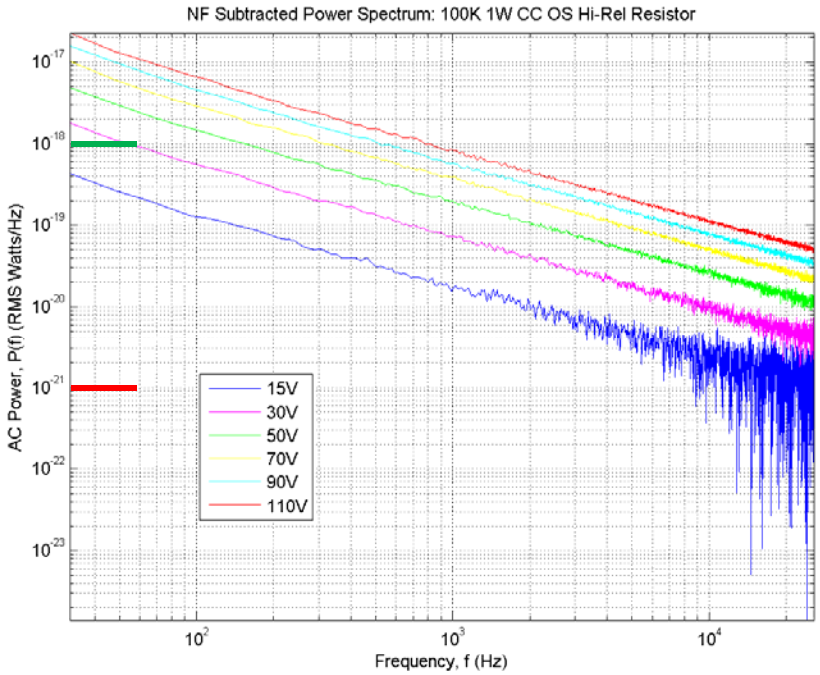

***Figure 4-2**: The noise power of the 100 kΩ 1-W OS CC Hi-Rel resistor. The power follows very closely with the noise spectrum, and the level of power is very small. The solid green line at 10^{-18} W/Hz represents the attowatt/Hz level, and the solid red line at 10^{-21} W/Hz represents the zeptowatt/Hz level.*

This graph represents the spectral noise power emitted by the $1/f$ noise in the resistor. As can be seen, the spectral noise power is on the order of attowatts/Hz (10^{-18} W/Hz) to zeptowatts/Hz (10^{-21} W/Hz).

Similarly, the output current can be obtained by using Ohm's law: $I = V/R$ where V is the RMS voltage and R is the resistance. The result of this calculation is shown in **Figure 4-3**.

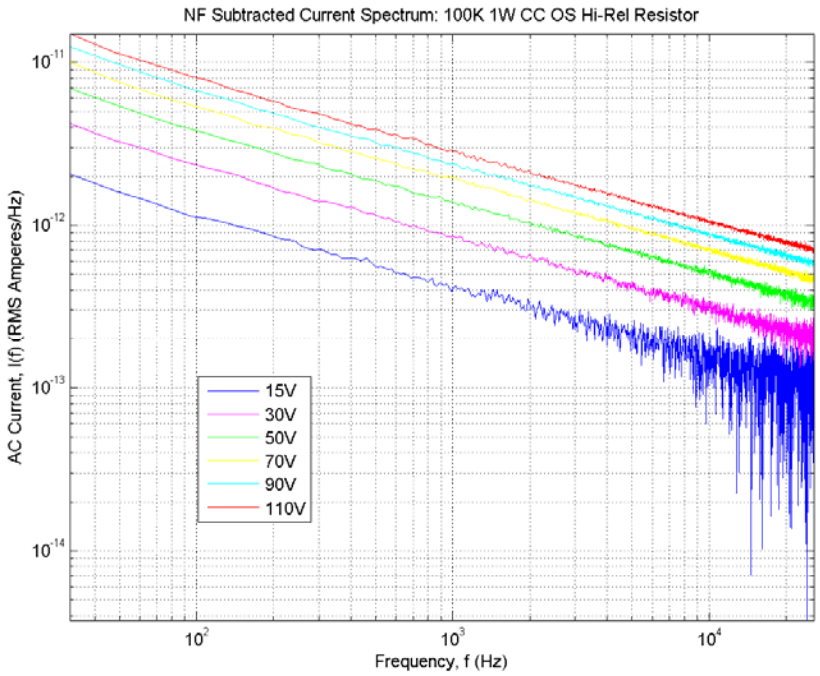

***Figure 4-3**: The noise current spectrum from the 1/f noise from the 100 kΩ 1-W OS CC Hi-Rel resistor. As can be seen, the level of output current is very small.*

The output spectral noise power and current have small levels, on the order of attowatts and picoamperes. These small of levels do not have much of an effect on the system. The result is interesting because from an applied dc voltage, the resistor can produce ac power and current.

IV.4. Comparisons of noise spectra

The noise spectra of the 1/f-noise producing resistors are compared. The largest 1/*f*-noise producing resistors are the OS CC resistors and the TF resistor. **Figure 4-4** shows a comparison of the noise spectra for all of the resistors.

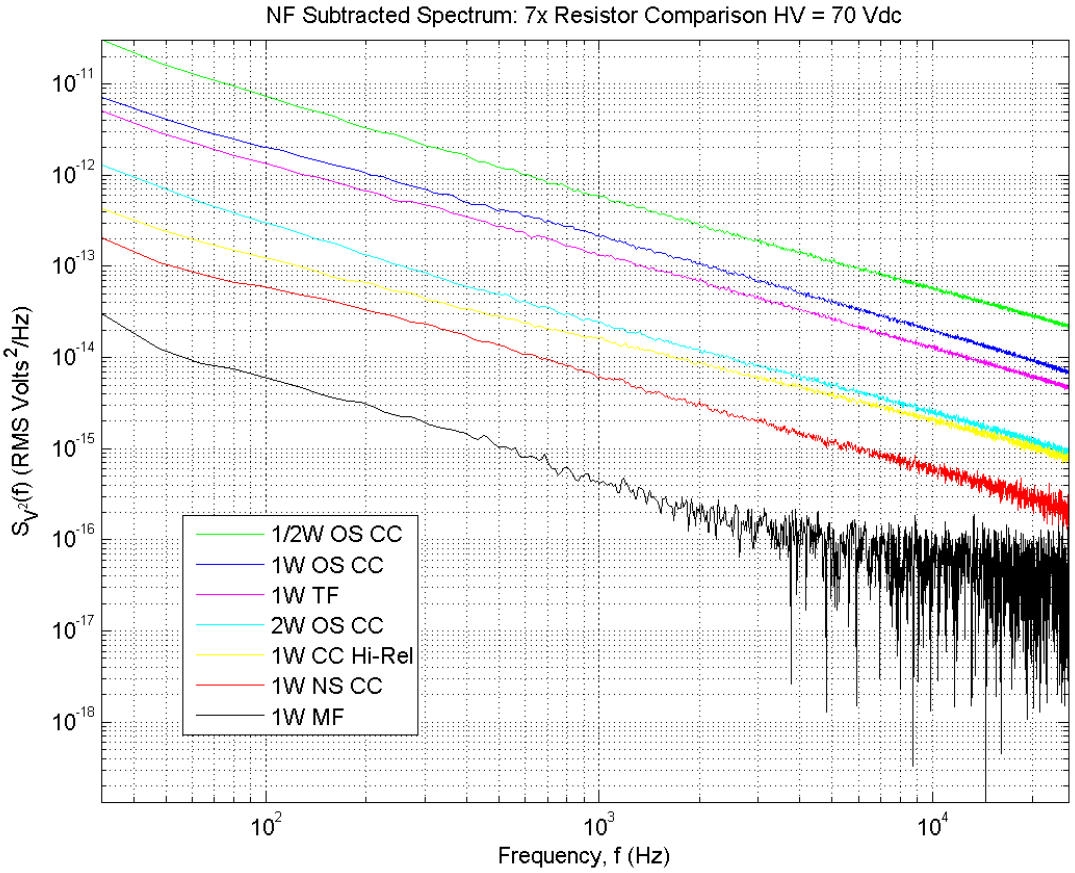

***Figure 4-4**: The noise subtracted spectra of all the 1/f noise producing 100-kΩ resistors at 70 V_{dc}. The 1/2-W CC resistor produced the most noise, and the 1-W MF resistor produced the least noise. The 1-W OS CC and the 1-W TF resistors produced comparable noise levels.*

Out of the CC resistors, the ½-W OS CC resistor produced the most noise and the 2-W OS CC produced the least 1/*f* noise along with the 1-W OS CC Hi-Rel resistor. Since the resistors of different power ratings are physically of different sizes, the level of noise brings to mind a volume dependence in the noise spectrum. Voss and Clarke [16] obtained results that showed that the noise spectrum was proportional to the inverse of the volume of the resistor. This result is consistent with the results obtained from this experiment to an extent. The volume of the 1-W OS CC Hi-Rel resistor is not physically bigger than the 1-W OS CC resistor, but the two resistors produce different levels of noise because internally, they are constructed differently (see **Figure 4-5**). The 1-W TF resistor is also much smaller than the CC resistors, but the noise produced is comparable to that of the 1-W OS CC resistor. The MF resistor also is of a comparable size to the 2-W OS CC resistor. Qualitatively, when comparing the OS CC resistors of different power ratings (and consequently different volumes) but same composition and manufacturing, the results of this experiment are consistent with that of Voss and Clarke's.

In addition, the noise spectra of the 1-W CC Hi-Rel and NS resistors are compared. Naively, the noise spectra of the two resistors are thought to be the same based on composition, resistance, etc.

However, **Figure 4-5** shows the manufacturing difference in the two resistors along with two other resistors.

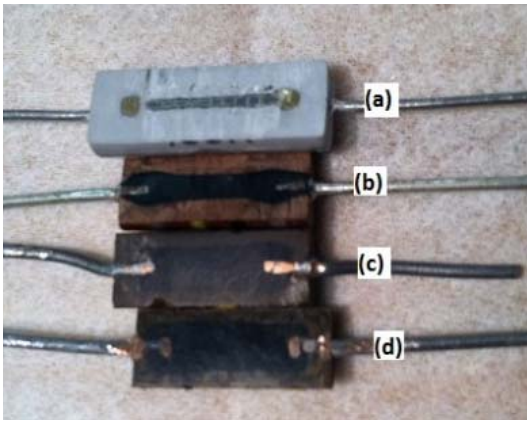

***Figure 4-5**: (a) The 100-kΩ 1-W MF resistor. (b) The 100-kΩ 1-W NS CC resistor. (c) The 100-kΩ 1-W OS CC resistor. (d) The 100-kΩ 1-W Hi-rel CC resistor.*

The carbon composition matrix is the material that the electrons flow through. An example of the 100-kΩ 1-W MF resistor is shown for completeness. In the NS CC resistor, the material goes out to the edge of the resistor, making some contact with the outside. However, in the OS CC resistor, the matrix is solely inside the resistor, and it makes contact with only the leads of the resistor. The carbon matrix in the OS resistor does not touch outside. The Hi-Rel resistor has plates inside the composition as opposed to just the leads in the OS resistor. The difference in manufacturing is likely the source of the difference in noise spectra of the two resistors.

In **Figure 4-6**, the noise spectra of the two 1-W CC resistors are compared.

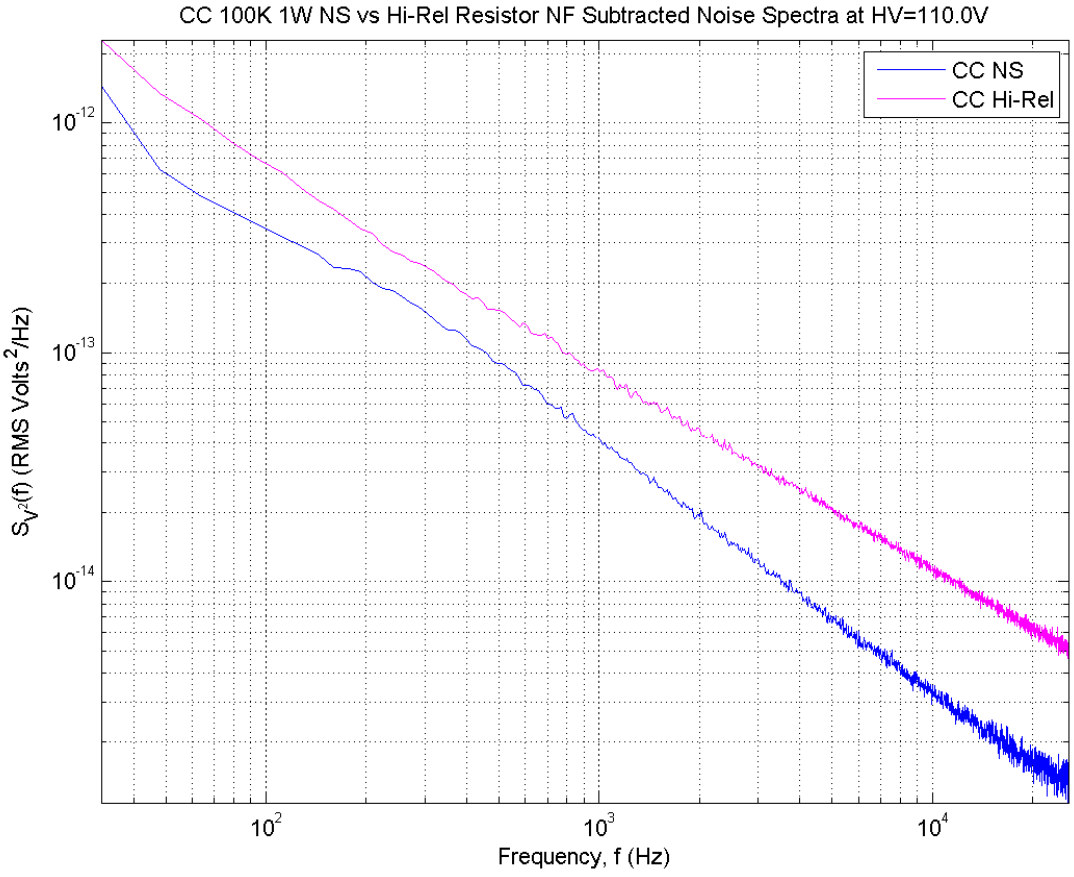

***Figure 4-6**: The noise spectra of the 1-W CC NS resistor vs. the 1-W CC Hi-Rel resistors at 110 V_{dc}. Here, the NS resistor deviates from 1/f near the low-end frequencies. In addition, the levels of noise are very different in the two resistors.*

The difference in the shape and levels of the noise spectra for the two resistors is obvious. Here, the NS CC resistor does not produce pure 1/*f* noise, while the OS CC resistor does. At low frequencies, the NS CC resistor experiences a bend, which marks a deviation from linearity on a log-log graph. The levels of noise are also different for the two resistors. As can be seen in **Figure 4-5**, the NS resistor has more volume of carbon composition than the OS resistor. The claim of the proportionality of the noise spectrum with the inverse of the volume can be made here as well.

IV.5. Universal Scaling in 1/*f* Noise

The universal scaling equation, which is a function of frequency and the dc voltage applied across the resistor under test, is obtained for each resistor via a 3-parameter least-squares fit to 6 noise spectra. In **Eq. 3-1**, the universal scaling spectrum is defined experimentally. The theoretical noise spectrum is given in **Eq. 4-2**:

$$U_{V^2}(f, V_{dc}) = \frac{S_{V^2}(f)}{V_{dc}^{\gamma}} = \frac{\alpha}{f^{\beta} V_{dc}^{\gamma}} \left[\frac{V_{rms}^2}{Hz} / V_{dc}^{\gamma}\right] \quad \textbf{(Eq. 4-2)}$$

where $S_{V^2}(f) = \frac{\alpha}{f^{\beta}}$. Here, $U_{V^2}(f, V_{dc})$ is obtained by fitting the data collected to the parameters in **Eq. 4-2**. This is done by minimizing the χ^2 values to the data. More explanation of this method is given in **Appendix 2**.

Each parameter in the universal scaling equation has its own physical meaning. Since we are plotting this function in log-log-log space, it is convenient to visualize the universal scaling in such space. Taking the $\log_{10}$ of **Eq. 4-2** gives **Eq. 4-3**:

$$Y(x, w) = a + bx - cw \quad \textbf{(Eq. 4-3)}$$

where $Y(x, w) = \log_{10} U_{V^2}(f, V_{dc})$ and represents the equation of a planar 2d surface, $x = \log_{10} f$, $w = \log_{10} V_{dc}$, $a = \log_{10} \alpha$, $b = -\beta$, and $c = \gamma$. Here, *a* is the intercept at x = 0 and w = 0. Thus, α represents the exponentiated intercept. Effectively, α is the noise when f = 1 Hz and V_{dc} = 1 V_{dc}. From **Eq. 4-3**, β is the dependence of the noise on the frequency. In 1/*f* noise, β should be ≈ 1. In addition, γ is the dependence of the noise on the dc voltage across the resistor. Naively, γ would be expected to have a value ≈ 2, but the experiment shows otherwise.

Least-squares fit calculations were performed to determine the parameters in the universal scaling function. Using the χ^2 method, estimates of each parameter is found, α^*, β^*, and γ^* as well as their uncertainties. The least-squares fit results for each resistor are shown in **Table 4-1**.

***Table 4-1**: Least-Squares Fit Parameters for Universal Scaling*

100 kΩ Resistors	α^*	β^*	γ^*
½-W OS CC	4.2889E-12 ± 4.1116E-16	0.9884 ± 0.000056	1.3766 ± 0.000126
1-W OS CC	1.5086E-13 ± 1.6668E-17	0.9979 ± 0.000066	1.8582 ± 0.000140
1-W OS CC Hi-Rel	5.3919E-15 ± 8.9060E-19	0.8723 ± 0.000104	1.8704 ± 0.000201
2-W OS CC	1.6224E-14 ± 2.3870E-18	0.9956 ± 0.000091	1.9761 ± 0.000180
1-W NS TF	3.3286E-14 ± 3.7613E-18	1.0268 ± 0.000068	2.2584 ± 0.000142
1-W NS CC	5.3026E-15 ± 1.2866E-18	1.0074 ± 0.000166	1.8872 ± 0.000293
1-W MF	8.7848E-16 ± 5.8888E-19	0.9629 ± 0.000570	1.7127 ± 0.000794

Not obvious from the table, α^*, β^*, and γ^* are correlated parameters. In short, if one of the parameters were to change, the other parameters would also be affected by this change. More discussion on these uncertainties is explained further in **Appendix 3**.

IV.6. Discussion of Noise from the 100-kΩ Resistors

Metal Film 100-kΩ Resistor

As can be seen in **Figure 3-8**, the metal film resistor exhibits 1/*f* noise at low levels. Compared with noise spectra from the other 1/*f* producing resistors, the level of the noise of MF resistors is much smaller. This result is puzzling because the MF resistor was expected to exhibit only Johnson-Nyquist noise. The noise floor subtracted data were quite noisy among the curves due to the low-level of 1/*f* noise present in the MF resistor. At high frequencies, the curves are almost indistinguishable. Investigations are still in progress as to the explanation of the 1/*f* noise present in these MF-resistor measurements. One explanation is the possibility of low-level leakage current from the blocking capacitors in the circuit, which would be HV-dependent.

Thick Film 100-kΩ Resistor

Shown in **Figure 3-9**, the thick film resistor produced 1/*f* noise. This phenomenon was expected. In addition, the γ value for this resistor is slightly greater than the naïve value of 2. This resistor was the only resistor to have a γ value greater than 2. The level of noise is on the same order of magnitude as the 1-W OS CC resistor.

1-W Old Stock High-Reliability Carbon Composition 100-kΩ Resistor

Shown in **Figure 3-10**, the 1-W OS Hi-Rel CC resistor produced 1/*f* noise. Again, this phenomenon was expected. Here, the β value in the fit was the furthest away from 1. Here, the β value

is approximately 13% away from 1/*f*. However, the universal scaling equation still holds. The level of noise is on the same order of magnitude as the 2-W OS CC resistor.

½-W Old Stock Carbon Composition 100-kΩ Resistor

Shown in **Figure 3-11**, the 1/2-W OS CC resistor produced 1/*f* noise. This resistor produced the most amount of noise as consistent with Voss and Clarke's [16] take on the size of the resistor having implications to the noise level. The γ value for this resistor was much different than the other γ values. This value is far off of the naïve value of 2. The V_{dc} curves are further apart for this resistor than for the other resistors. Since there is a strong correlation among the parameters in the universal scaling, the relatively high value for the α value corresponds with a low γ value.

1-W Old Stock Carbon Composition 100-kΩ Resistor

As can be seen in **Figure 3-12**, the 1-W OS CC resistor shows 1/*f* noise. The γ value is slightly less than that for the γ value for the 2-W OS CC resistor and is relatively larger than the γ value for the 1-W OS CC resistor. The noise levels are comparable to the TF resistor as well as the β values, but the γ values are different.

2-W Old Stock Carbon Composition 100-kΩ Resistor

In **Figure 3-13**, the spectrum for the 2-W OS CC resistor shows 1/*f* noise. The level of the noise is the lowest for the 1/*f*-noise producing CC resistors along with the 1-W Hi-Rel resistor, and thus has a low α value. The parameters agree well with the theory compared with the other resistors.

1-W New Stock Carbon Composition 100-kΩ Resistor

The noise spectrum for the 1-W NS CC resistor showed slight deviations from 1/*f* noise, as can be seen in **Figure 3-14**. In the low frequency range, the spectrum shows a bend in the data. The expectation for the 1/*f* noise is that on a log-log plot, the spectra should be linear. However, in the case of the 1-W NS CC resistor, the data show nonlinearities (the bend) from 1/*f*. However, the spectra measured at different V_{dc} are still parallel, and do line up when fitted with a universal scaling as in **Eq. 3-1**. In this case, the γ value is ≈ 1.90. This means that the noise spectrum, $S_{V^2}(f)$, of the 1-W NS CC resistor is still dependent on the high voltage applied to the resistor.

V. Conclusions

V.1. Major Activities

Noise spectra from seven different resistors were measured. First, a circuit was built to measure the noise in a resistor under test as shown in **Figure 2-1**. High voltages were applied to the 100-kΩ MF resistors. The dc voltages applied across the resistor under test were 15 V, 30 V, 50 V, 70 V, 90 V, and 110 V. The differential signal from the AD624 op-amp was read in by the Agilent 35670A DSA. The DSA performs an autocorrelation of the differential voltage noise signal to express the noise as in **Eq. 2-3**. Various noise-cancellation techniques were implemented to cut down on the ambient electromagnetic noise in the room. These techniques took some time to figure out, which limited the number of

resistors that could be tested in the time available. Putting the circuit into a metal box, nitrogen inerting that box, and minimizing the noise based on the orientation of the cables were used to minimize the ambient noise.

V.2. Significant Results

The NS CC did produce 1/*f* noise, but not a perfectly straight line relation on a log-log plot. The other resistors that were tested did. As was predicted, the OS CC resistors of the ½-W, 1-W, and 2-W power ratings produced 1/*f* noise. These OS CC resistors were known to produce 1/*f* noise. The 1-W OS CC Hi-Rel resistor also produced the expected 1/*f* noise. The TF resistor produced 1/*f* noise as well, which was predicted. However, the MF resistor produced low levels of 1/*f* noise, which was not expected. This result is still being investigated. The MF resistor was expected to produce only Johnson-Nyquist thermal noise, which is flat with frequency. The NS CC resistor was not expected to deviate from 1/*f* noise at first, but after examining the noise spectra, further reading of literature was carried out and confirmed that the NS CC resistor would not produce perfectly linear power law 1/*f* noise.

The γ values for the resistors also varied. The ½-W CC resistor had the smallest γ value, while the TF resistor had the highest γ value. In **Table 4-1**, the values of α, β, and γ corresponding to the parameters in **Eq. 4-2** are presented.

V.3. Comparison of Noise Spectra

The ½-W CC resistor produced the most 1/*f* noise, while out of the CC resistors, the 1-W OS CC Hi-Rel resistor and the 2-W CC resistor produced the least 1/*f* noise. The 1-W MF resistor produced the least amount of 1/*f* noise. The 1-W OS CC and 1-W TF resistors had comparable noise levels. However, the resistors having similar noise levels at 70 V_{dc}, as shown in **Figure 4-4**, do not necessarily have similar parameters for the universal scaling spectrum. In addition, the comparison of the two 1-W CC (OS and NS) resistors presented in **Figure 4-6** shows the deviation of the noise produced by the NS CC resistor from 1/*f* noise.

V.4. Future Work

In the future, the noise from a resistor exposed to a humid environment will be investigated. Initial measurements of the 1-W OS CC Hi-Rel resistor exposed to a humid environment have been made. However, the analysis of the measurements has not been completed. Because the circuit was immersed in a nitrogen-inerted environment, the humidity associated with the resistor was assumed to be minimized. Separate resistors left out of the nitrogen-inerted box were exposed to 50-60% relative humidity on a daily basis.

In addition to the experimental work, a 1/*f*-noise-producing guitar effects pedal will be constructed in the future. Since 1/*f* noise is aesthetically pleasing, building a guitar effects pedal to produce 1/*f* noise could have some musical applications. The Zener diode produces 1/*f* noise when reverse-biased at its breakdown voltage. A Zener diode will be used with an analog voltage multiplier to build a stereo effects pedal. The aim is to produce as much 1/*f* noise as possible to capitalize on the musicality of it.

VI. Acknowledgments

I thank Professor Steve Errede for his valued time, energy and efforts towards this project as well as his invaluable lessons. I also thank Annelise Roti Roti for valuable discussions and Celia Elliott for her advice and lessons. This work was supported in part by the Lorella M. Jones Undergraduate Research Award of the Department of Physics, University of Illinois at Urbana-Champaign.

VII. References

[1] Imperial College, EE 3.02/A04 Instrumentation. "2. Noise", Autumn 2008.

[2] Tim J. Sobering, Noise in Electronic Systems, Technote 4, SDE Consulting, May 1999.

[3] Nichols A. Romero, Johnson Noise, Junior Physics Laboratory, Massachusetts Institute of Technology, Cambridge, Massachusetts 02139, November 26, 1998.

[4] Edoardo Milotti, *1/f* noise: a pedagogical review. Dipartimento di Fisica, Universitá di Udine and I.N.F.N. – Sezione di Trieste. Via delle Scienze, 208—I-33100 Udine, Italy.

[5] P. Dutta and P.M. Horn. Low-frequency fluctuations in solids: 1/*f* noise. Reviews of Modern Physics, Vol. 53, No. 3, July 1981.

[6] Richard F. Voss and John Clarke, J. Acoust. Soc. Am. **63** (1), Jan. 1978.

[7] Christopher T. Kello et. Al, Cognitive Science. 32 (2008) 1217-1231.

[8] Peter M. Marchetto, 1/*f* and Johnson-Nyquist Noise in metal-film and carbon resistors, Bioacoustics Research Program, Cornell Lab of Ornithology, Cornell University, Ithaca, NY.

[9] Analog Devices: Rarely Asked Questions (RAQs) : Resistors in Analog Circuitry [Online]. http://www.analog.com/static/imported-files/rarely_asked_questions/moreInfo_raq_resistors.html [10/17/14].

[10] Analog Devices, "Precision Instrumentation Amplifier," AD624 datasheet, 1999.

[11] S. M. Errede, *P406POM Lecture 13 Part 2.* UIUC Physics Dept, 2014. https://courses.physics.illinois.edu/phys406/Lecture_Notes/P406POM_Lecture_Notes/P406POM_Lect13_Part2.pdf.

[12] Agilent Technologies, *Agilent 35670A Operator's Guide*, Agilent Technologies, Inc, 1992-2010.

[13] Ryan Hurley. (June, 2005). Design Considerations for ESD/EMI Filters: I [Online]. Literature Distribution Center for ON Semiconductor. http://www.onsemi.com/pub_link/Collateral/AND8200-D.PDF [10/17/14].

[14] H. Nyquist, Phys. Rev. 23, 110 (1928).

[15] Peter M. Marchetto. *1/*f *and Johnson-Nyquist Noise in metal-film and carbon resistors*. Bioacoustics Research Program, Cornell Lab of Onithology, Cornell University, Ithaca, NY.

[16] Richard F. Voss and John Clarke. Phys. Rev. B **13**, 2 (1976).

Appendix 1 – Correcting the Noise

Stray Capacitance

Stray capacitance is a small, but real capacitance associated with the inputs of the AD624 op-amp. The leads at the ± inputs act as conductors, and geometrically form a capacitance. The dielectric is air, which is approximated as a vacuum. The stray capacitance, C_s, simply short-circuits ac signal to ground at high frequencies. This phenomenon describes for instance in **Figure 3-5** where the noise spectrum drops off at high frequencies for the measurements made with the AD624 circuit. Determining the stray capacitance and applying it to the data straightens the non-frequency-dependent thermal noise. A least-squares fit program was written to determine the stray capacitance value, which computed $C_s = 60.6 \pm 0.2$ pF.

Resistor Noise Transfer Function

Each resistor in the circuit shown in **Figure 2-1** acts as a voltage noise source based on its thermal noise, and for Rdut, the $1/f$ noise. The noise voltage produced by any resistor is loaded down by the presence of the other components in the circuit (resistors, capacitors). The AD624's input impedance is $10^9\ \Omega$, and thus was neglected. The 2 μF blocking capacitors and the stray capacitances have imaginary impedances, which are associated with their reactances. These capacitances can store energy, which acts as a voltage drop. Because of these effects, the actual level of noise produced by the Rdut is higher than what is measured by the DSA. Each of the resistors has a transfer function, which is the percentage of the measured noise associated with its intrinsic noise. The magnitudes of each of the transfer functions, H, were added in quadrature to equal 1. The contribution of all the components of the circuit equals the total measured noise.

The magnitude of the transfer function for the Rdut was ≈ 40%. This is to say that 40% of the total noise from Rdut was the measured noise. A plot of the magnitude of the transfer function squared as a function of frequency for Rdut is shown in **Figure 1**. In order to correct the noise spectra, the voltage noise had to be divided by the magnitude of the transfer function. Although H is a function of frequency, f, the transfer function for the range of measurements for $1/f$ noise was approximately constant, except at higher frequencies.

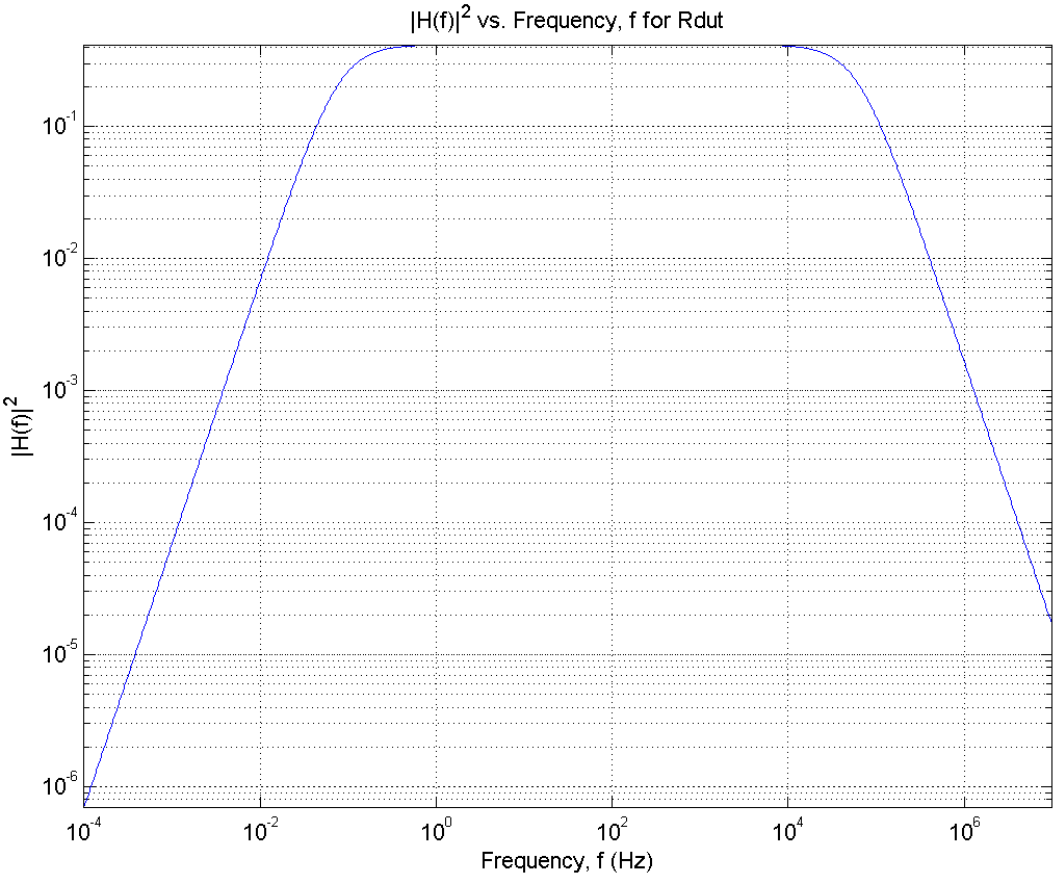

***Figure 1**: The magnitude of the transfer function squared for the 100-kΩ Rdut as a function of frequency. The transfer function falls off at high frequencies.*

Appendix 2 – Determining Best Fit Parameters

Determining the noise parameters

The universal scaling equation is expressed by **Eq. 4-2**, which contains three parameters, α, β, and γ. Each of these parameters was found by way of minimizing χ^2 distribution associated with the resistor spectral noise data. It was convenient to work first with minimizing the χ^2 for a straight line fit represented by **Eq. 4-3**. The parameters, a, b, and c were then associated with the parameters α, β, and γ. Wherever the χ^2 showed a minimum over the range of each parameter was the best fit value for the parameter.

Statistical Uncertainties

Minimizing the χ^2 distribution also provides a method for determining the uncertainties associated with fitted parameters. The change in the χ^2 by a value of 1 corresponds to a 1-σ uncertainty range. For example, **Figure 2** shows the $\Delta\chi^2$ minimization of the χ^2 as a function of the a parameter for

the Hi-Rel resistor. The $\Delta\chi^2$ value represents the difference between the value of the χ^2 and the χ^2 minimum value.

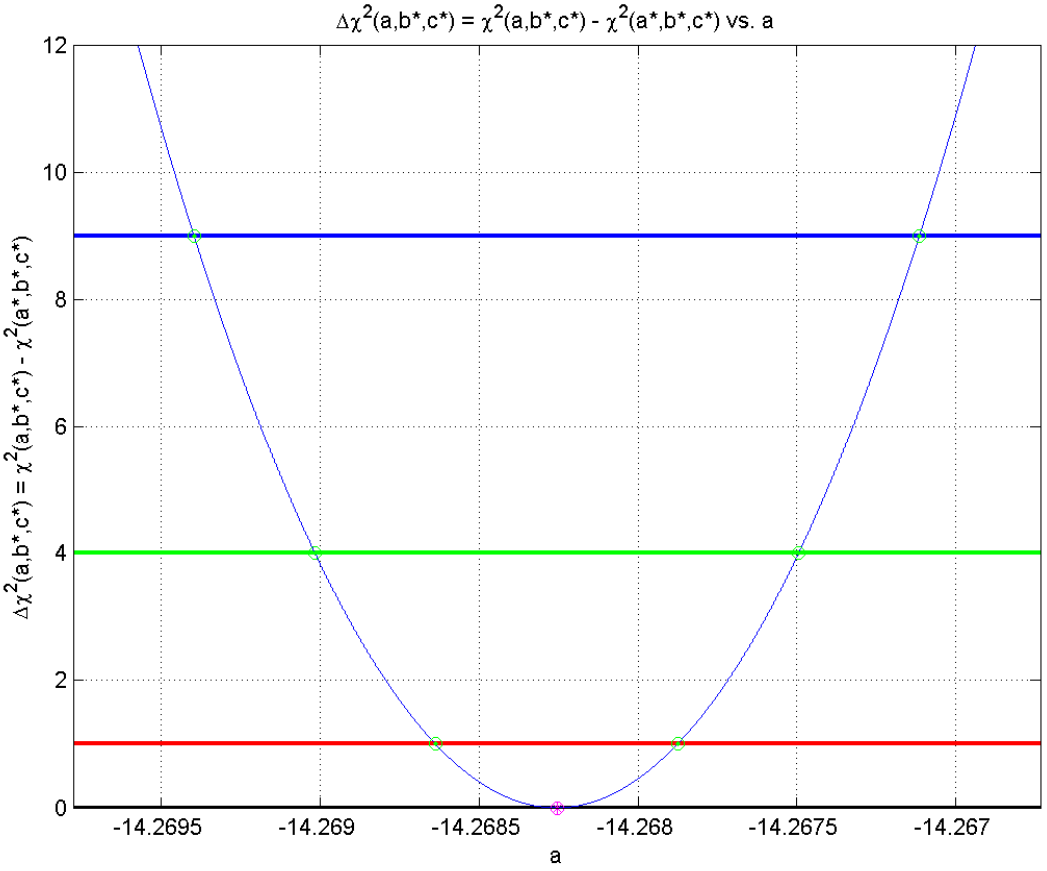

***Figure 2**: The $\Delta\chi^2$ distribution as a function of a. The red line represents the 1-σ uncertainty, the green line represents the 2-σ uncertainty, and the blue line represents the 3-σ uncertainty.*

In addition to determining the values of uncertainty this way, the parameters were highly correlated. **Figure 3** shows the correlation between the *a* and *b* parameters in the same resistors. The more elongated and less circular the distribution is, the more correlated or anti-correlated they are. If the slope along the elongated side were positive, a positive correlation would exist.

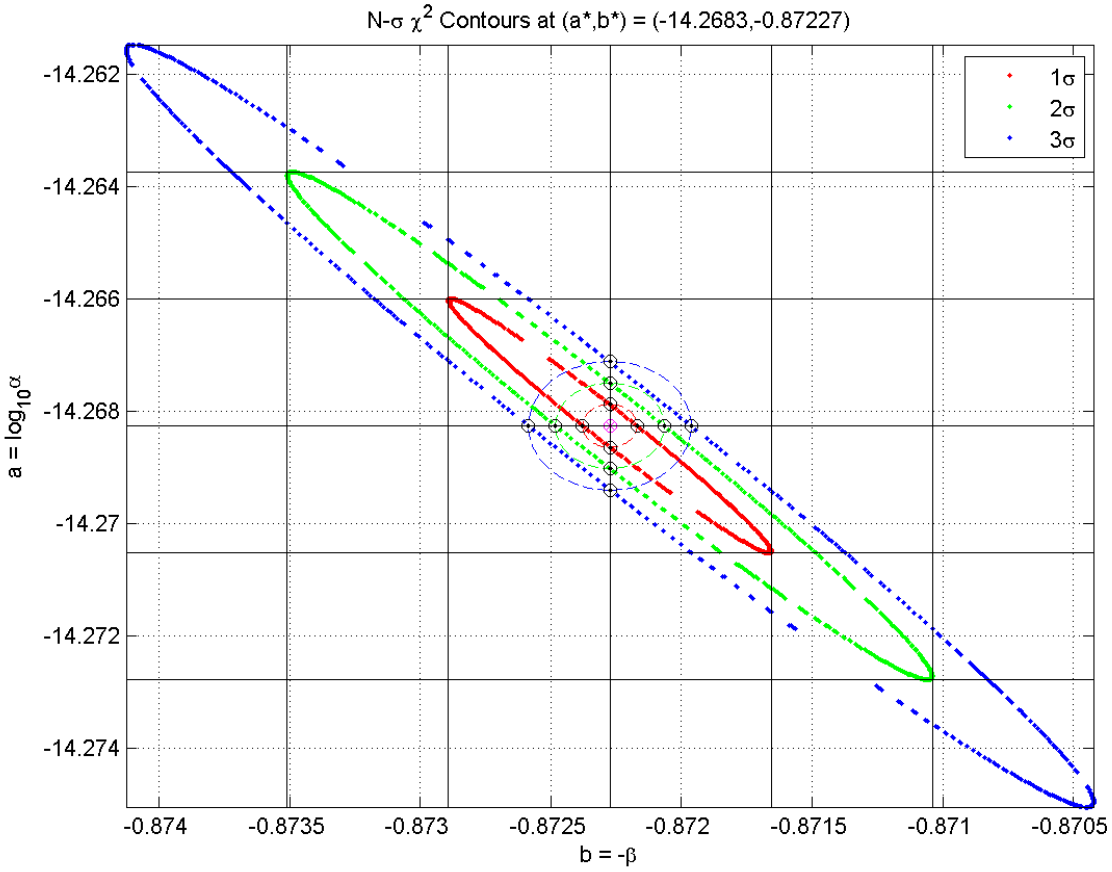

***Figure 3**: The contours of the uncertainties while varying each parameter. The circled contours represent sweeping over a χ^2 while holding all other parameters fixed.*

In reality, the three parameters all play a part with each other. Correlations exist among all three parameters. In **Figure 4**, the 3D contours show how each parameter is correlated with itself. The red surface represents the 1-σ uncertainty, the green surface represents the 2-σ uncertainty, and the blue surface represents the 3-σ uncertainty.

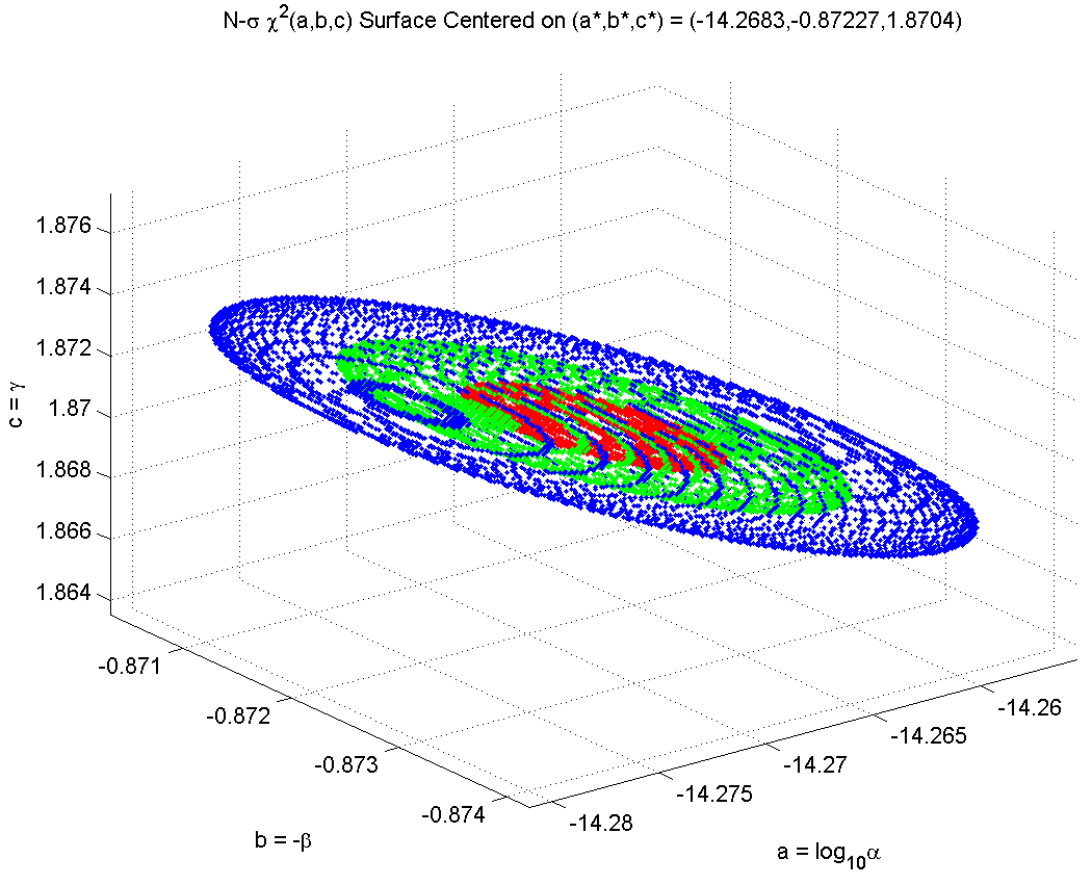

***Figure 3**: Contour of the correlational uncertainties in the parameters a, b, and c. The red surface represents 1 σ, the green surface represents 2 σ, and the blue surface represents 3 σ.*

Appendix 3 – Absolute Calibration of the DSA and gain of AD624 op-amp

DSA Calibration

An absolute calibration of the DSA was made to ensure the quality of the measurements. The SRS 830 lock-in amplifier acted as a function generator that produced a sine wave at 1.000 V_{rms} with frequency 1024.0 Hz. The DSA had a Δf value of 32.0 Hz. Two Fluke 189 voltmeters were used to take initial measurements. Two initial measurements were taken: the input voltage in V_{rms} and mV_{rms}. The two measurements were not exactly the same, as the ratio of the mV measurement to the V measurement was 1.00150 ± 0.0000035. A second time, the LF411 unity gain buffer driver was placed on the output of the lock-in amplifier and the same measurements were made. These measurements agreed to the precision of the voltmeters.

Subsequently, the DSA was measured for calibration. Since the noise is spread among various frequency bins because of the discrete nature of the DSA, 5 frequencies were measured: 960, 992, 1024,

1056, and 1088 Hz. Multiplying the noise by the Δf value gives the value of V^2_{rms}. The signal from the lock-in amplifier directly was first used. The unity gain buffer driver was used in the next measurement. Adding the contributions from the 5 frequencies and taking the average of the ratios of the output to the input gives the absolute calibration of 1.00429 ± 0.00096.

AD624 Gain Calibration

A similar approach was used for measuring the calibration of the gain of the AD624. The gain of the op-amp was hard-wired at 100. The signal from the lock-in amplifier was 0.040 V_{rms} with a frequency of 1024.0 Hz. The two voltmeters measured the input signal from the lock-in amplifier in addition to the output of the AD624 gain. After taking the ratio of the output to the input and taking the average of the measurements from the two voltmeters, the AD624 was shown to have a gain of 100.1724 ± 0.0064.